# Biosensing with polydiacetylene materials: structures, optical properties and applications

**Mary A. Reppy*[a] and Bradford A. Pindzola[b]**

***Received (in Cambridge, UK) 12th March 2007, Accepted 13th June 2007***
***First published as an Advance Article on the web 11th July 2007***
**DOI: 10.1039/b703691d**

Polydiacetylene (PDA) materials are used as a platform for detection of biological analytes such as microorganisms, viruses and proteins. The environmentally responsive chromic and emissive properties of the polymer, combined with self-assembled material formats, make these materials particularly attractive for biosensing applications. A variety of approaches have been used in developing these materials and demonstrating their potential for biological detection. In this feature article we describe different PDA material formats, discuss the optical properties that are the basis for signal generation, and review the use of PDA for biosensing.

## 1 Introduction

Polydiacetylene (PDA) is a conjugated polymer with interesting and useful optical properties that have formed the basis for detection of biological entities. The advantages of PDA materials for sensing applications arise from their fortunate conjunction of environmentally sensitive optical characteristics and easy formation in self-assembled systems. Diacetylene amphiphiles will self assemble into a variety of forms that can be modified to incorporate ligands and substrates for detection applications, and be photopolymerized to generate PDA *in situ*. PDA, in turn, provides built-in optical signal generation arising from changes in the absorption and emission spectra of the conjugated backbone caused by target interaction with the materials.

There has been extensive research and development on PDA materials since their first preparation by Wegner in 1969.[1] The early work on the formation of PDA films and liposomes has been previously reviewed in 1985 by Tieke[2] and was the subject of a NATO Advanced Research Workshop.[3] Charych and colleagues and Ribi and co-workers were the first to begin using PDA materials for biosensing applications in the early 1990s. The work of the Charych group was reviewed in 1998;[4] the work of Ribi is presented in several patents.[5,6] The chromic transitions and nanomechanical properties of PDA thin films were briefly reviewed in 2004.[7] Other reviews have touched on PDA liposomes in discussion of polymerized liposomes[8,9] and have compared them to other conjugated

[a]*Analytical Biological Services, 701-4 Cornell Business Park, Wilmington DE, USA. E-mail: reppy@alum.mit.edu*
[b]*Currently at TIAX, LLC 15 Acorn Park, Cambridge, MA, USA. E-mail: pindzola.brad@tiaxllc.com*

**Mary A. Reppy**

*Mary Reppy received her undergraduate degree in Chemistry from the Massachusetts Institute of Technology in 1987. She worked for two years with Professor Feigenson at Cornell University in liposome research before beginning graduate research in physical organic chemistry with Professor Charles Wilcox Jr, on polycyclic aromatic and anti-aromatic hydrocarbons. She received her PhD in Chemistry from Cornell University in 1994 and became a post-doctoral fellow at the Polymer and Electrochemistry Center of SRI International in Menlo Park CA, developing polymer systems for sensing applications. She then became a post-doctoral fellow at University of California at Berkeley with Professor Douglas Gin working on imprinted polymers and polymerizable lyotropic liquid crystals (LLCs) with nanoscale dimensional control. She joined Analytical Biological Systems in 1999, directing a research program on the development of novel fluorescent polydiacetylene (PDA) materials for bio-sensing and assay applications, where she pioneered the use of energy transfer from PDA to fluorophores for signal amplification and discovered new methods for preparing PDA coatings on porous supports. Her research interests include the design of bio-organic hybrid nanostructured materials for sensing and assay applications.*

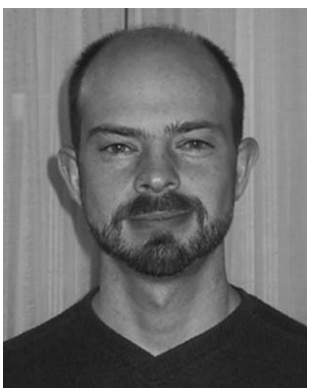

**Bradford A. Pindzola**

*Brad Pindzola received his undergraduate degree in Chemistry from Carleton College in 1997. He received his PhD in Chemistry from the University of California at Berkeley in 2001, working on the design and synthesis of polymerizable amphiphiles for the in-phase polymerization of lyotropic liquid crystals with Professor Douglas Gin. He then joined the research effort at Analytical Biological Services, developing polydiacetylene materials for the detection of biological targets and the analysis of small molecules. In April 2007 he started as a Senior Research Chemist at TIAX, LLC in Cambridge, Massachusetts.*

polymer sensors.[10] A recent short review focused on formation of PDA nanowires.[11]

Recently, there has been an increase in the number and diversity of research efforts in the area of PDA materials, particularly for biosensing applications. Additional material formats have been explored, including SAMs, multilayer coatings and surface immobilized liposomes. The mechanisms of chromic and fluorescence change continue to be investigated and the potential application of these materials for detection of microorganisms, proteins and small molecules has been demonstrated. PDA research draws from many diverse fields: photophysics, polymer chemistry, self-assembly, colloids, and biochemistry. Researchers from these different fields have contributed greatly to the understanding of these materials, but differences in approach and terminology have also hampered progress. In this feature article we discuss critical aspects of PDA materials, their implications for the development of sensing platforms and summarize recent work on biodetection using PDA.

## 2 Polydiacetylene materials

### 2.1 Diacetylene structures and polymerization

PDA is formed from the 1,4-photopolymerization of diacetylenes, which forms a conjugated backbone with side chains (Scheme 1). The polymerization only proceeds when the diacetylenes are arranged in a lattice with appropriate geometry and the propagating species is believed to be a dicarbene.[12] This topochemical constraint means that polymerization can only occur in solids or other highly ordered structures. Polymerization of self-assembled monomers leads to physical stabilization of the structure, increasing thermal stability and mechanical strength.[13]

PDA is colored, with hues from blue to red to yellow. Extended exposure to UV light usually causes a shift to lower wavelength absorbances in PDA materials (*e.g.*, blue to red) and can cause depolymerization and chain scission.[14,15] Some PDA systems actually develop absorbance at higher wavelengths with extended UV exposure,[16] however; these systems are usually characterized by overall weaker polymerization. Fig. 1 shows the effect on the absorbance spectra of two different fatty acid liposomes of extended irradiation. 5,7-TCDA liposomes require much higher UV doses than 10,12-PCDA liposomes to form significant amounts of polymer, as shown by the difference in absorbance intensities. Early in the

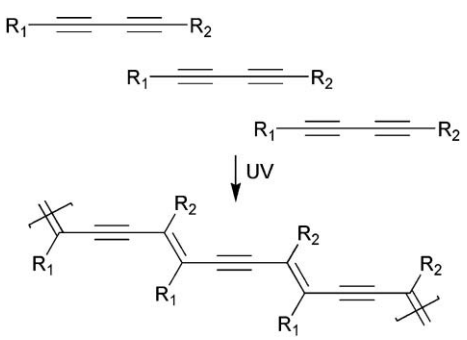


**Scheme 1** Topochemical photopolymerization of diacetylenes.

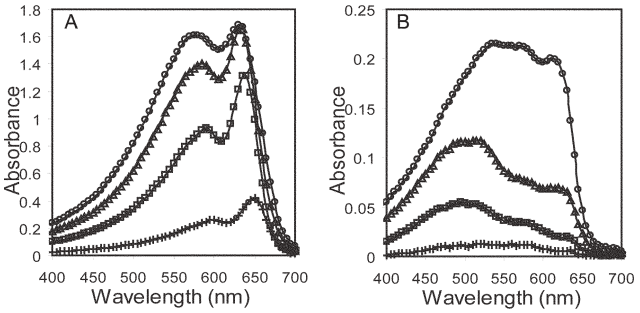


**Fig. 1** UV-vis absorbance spectra of PDA liposomes. (A) 10,12-PCDA and (B) 5,7-TCDA. Liposomes were prepared in water at 1 mM lipid by probe sonication, cooled at 10 °C and polymerized with 0.1 (+), 0.4 (□), 1.2 (△) and 2.0 (○) J $cm^{-2}$ 254 nm light.

polymerization of PDA, absorbance below 550 nm dominates; this can be seen in 10,12-PCDA liposomes only at very low UV doses, but is obvious with the poorly polymerizing 5,7-TCDA liposomes. Further UV exposure leads to increases in absorbance above 600 nm with the liposomes turning blue, but with even more exposure the material becomes red againwith absorbances below 550 nm dominating.

The PDA backbone is usually represented as having alternating double and triple bonds (ene-yne), sometimes in resonance with a butatriene structure (Scheme 2). Raman spectroscopy,[17,18] X-ray studies[19,20] and $^{13}C$ NMR[21–23] all support the backbone as having primarily ene-yne character. Early on, it was proposed that the blue form of the polymer has the ene-yne and the red form the butatriene structures,[24] however, this theory has been largely discounted on theoretical,[25,26] as well as experimental grounds.[27]

Diacetylene monomers for self-assembled materials are composed of two parts: a polar headgroup and a hydrophobic tail containing the diacetylene moiety. Diacetylenes are usually prepared using the Cadiot–Chodkiewicz reaction consisting of the Cu(I) catalyzed coupling of an acetylene and a haloacetylene.[28] A large variety of monomers have been synthesized with different polar headgroups and tail structures; some representative examples are shown in Scheme 3 (**1–5**). The hydrophobic portion of the amphiphile is generally composed of a single alkyl chain, but can also have multiple chains with a diacetylene group in one or more chains. Each tail can be broken down into three parts: the diacetylene group, a spacer between the headgroup and the diacetylene, and the terminal alkyl chain. Bolaamphiphiles are an exception; they are membrane spanning with the two headgroups at the aqueous interfaces and the chain(s) linking the headgroups forming the hydrophobic region.

Each element of the diacetylene amphiphile plays a crucial role in determining if an amphiphile will form a self-assembled material and, if it does, what properties that material will have. For instance, headgroup chirality strongly influences colloidal


**Scheme 2** Possible resonance structures of PDA.

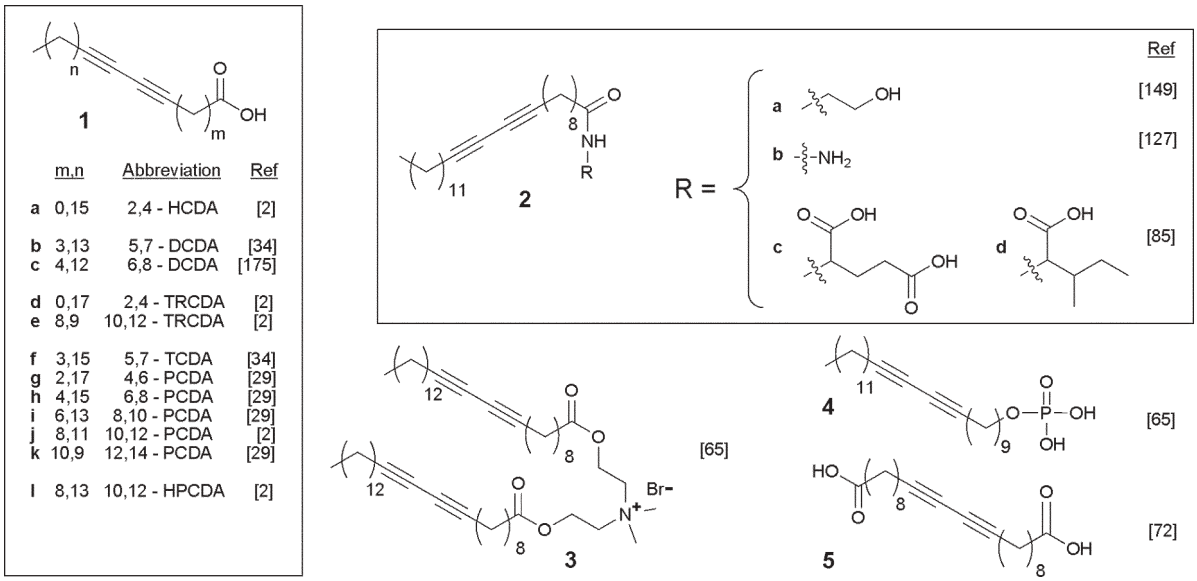


**Scheme 3** Diacetylene structures.

structure; amphiphilic monomers with achiral headgroups usually form spherical liposomes, whereas chiral amphiphiles often form non-spherical structures such as helices and tubules. The number and length of the tails largely controls the range of conditions under which an amphiphile will undergo self-assembly and the temperature of the melt transition ($T_m$) from "crystalline" chain packing to "liquid" chain packing.

**2.1.1 Diacetylene position and polymerization.** One very interesting question with respect to self-assembled diacetylenes is how the position of the diacetylene relative to the headgroup affects the packing and polymerization of the monomers. Several groups have investigated the impact of this parameter on formation and polymerization of LB films,[16,29] and SAMs.[30] Studies by Tieke and Lieser[16] and Tachibana *et al.*[29] on diacetylene fatty acid LB films showed that the location of the diacetylenes affected the film stability and polymerization. As the diacetylene was moved closer to the headgroup the observed collapse pressures increased, indicating more stable films, but the extent of polymerization decreased and the generated polymer was red or yellow rather than blue. For example, 8,10-; 10,12-; and 12,14-PCDA on an aqueous subphase with $Cd^{2+}$ all polymerized blue and converted to red with extended UV irradiation, while 6,8-PCDA polymerized red and 4,6-PCDA polymerized weakly yellow.[29] FTIR and XRD were used to estimate diyne tilt angle based on the CPK model. The three that polymerized blue had angles around 45°, close to that observed in crystalline diacetylenes. The angle in red-polymerizing 6,8-PCDA was much smaller, around 18°, and in the yellow 4,6-PCDA was much larger, around 70°.

Evans and co-workers also investigated the effect on polymerization of diacetylene position in studies using SAMs of diacetylene thiols on gold.[31] As with the films, moving the diacetylene moiety closer to the headgroup was seen to reduce polymerization. Shortening the overall chain length, while holding the position of the diacetylene relative to the headgroup constant, led to more red character in the polymer. A second study explored the influence of odd and even numbers of methylene units in the spacer between the diacetylene and the thiol.[30] Grazing-angle FTIR was used to show that all unpolymerized diacetylene monolayers were highly crystalline, but those with even spacers were relatively more disordered than those with odd spacers. Only the even spacer diacetylene monolayers produced significant quantities of blue character PDA as determined by resonance Raman spectroscopy, and shorter even-spacer monomers polymerized more poorly than longer even-spacer ones. These studies all indicate that a shorter spacer leads to better packing of the amphiphiles but poorer polymerization, and that an even spacer gives PDA with more blue character.

## 2.2 Material forms

Self-assembled PDA materials have been prepared in many different forms. These forms can be divided into five different classes: Langmuir, LB, and LS films; SAMs; multilayer coatings; colloids; and immobilized colloids (Fig. 2). Work with PDA in Langmuir and LB films through 1985 was thoroughly reviewed by Tieke;[2] this review includes an extensive list of diacetylene monomers. Here we will discuss subsequent work in those areas as well as new work in PDA liposomes, SAMs, multilayer coatings and immobilized colloids.

**2.2.1 Films and coatings.** Langmuir films and SAMs provide well-controlled platforms for studying fundamental aspects of PDA materials. PDA coatings are relatively easy to prepare compared to Langmuir films and SAMs, though with less control of structure and have recently shown utility in biosensing applications.

*2.2.1.1 Langmuir, LB, and LS films.* Langmuir films are formed by spreading amphiphilic molecules at an air/water interface and compressing them into close-packed arrays.

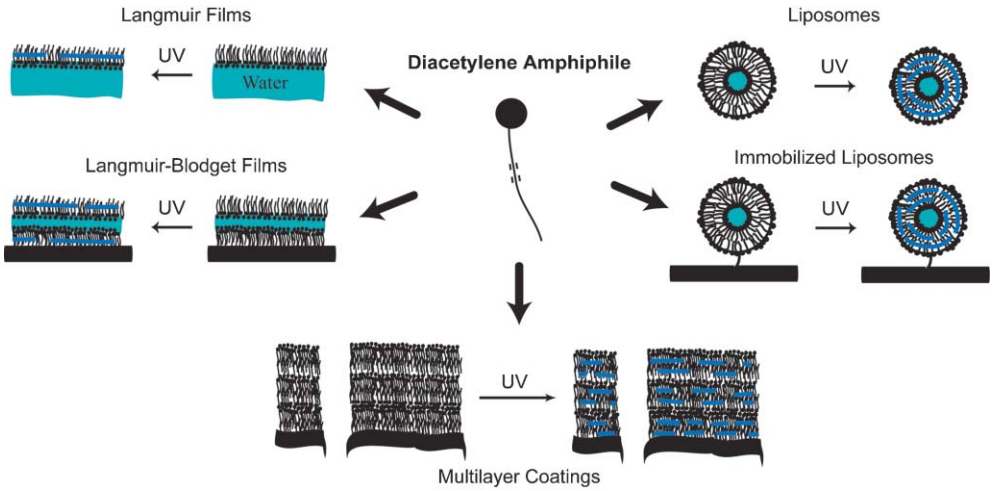


**Fig. 2** Diacetylene amphiphiles with a polar headgroup and diacetylene tail(s) form a variety of self assembled structures that can be photopolymerized.

These films can be studied at the air/water interface or transferred to a variety of solid supports to make LB, LS or similar films. PDA Langmuir films have been prepared on pure water subphases, as well as on mono- and divalent cation solutions. Langmuir films are a useful form for both spectroscopic and microscopic studies; such studies have shed much light on the structural characteristic of PDA materials.

Diacetylene fatty acid films are frequently prepared on $CdCl_2$ solutions; the presence of $Cd^{2+}$ can increase film stability[32] but also decrease the extent of polymerization.[16] Since the early review by Tieke, films have been prepared from new diacetylene monomers[33,34] and mixtures of diacetylenes and phospholipids, and additional work has been done on improving film quality. These efforts are briefly reviewed here.

There has been increasing interest in preparing PDA materials from mixtures of diacetylenes and other lipids to increase the biomimetic character of the materials. Leblanc and co-workers have studied mixed 10,12-PCDA systems,[35] including preparing a mixed monolayer of 10,12-PCDA with and a mannoside derivative (Scheme 4, **6**) at the air/water interface.[36] Using surface pressure–area isotherms and BAM, the authors concluded that the two components are miscible and identified three domains: one liquid expanded, and two condensed phases. The monolayers could be polymerized in

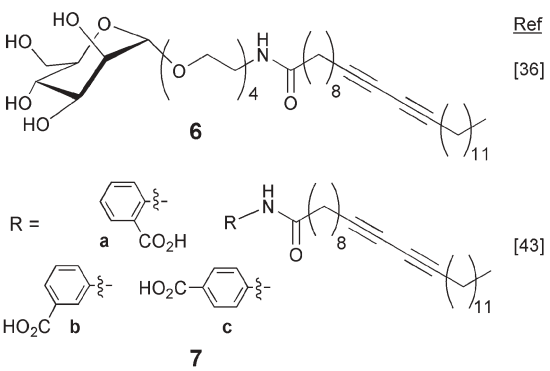


**Scheme 4**

both of the condensed phases, though increasing the fraction of **6** resulted in formation of red phase PDA and eventually disrupted polymerization entirely.

Jelinek and co-workers subsequently studied mixed diacetylene/phospholipid films. Langmuir films composed of 10,12-TRCDA with increasing percentages of DMPC were examined by pressure/area isotherm and poly(10,12-TRCDA)/DMPC LS films by PLM, and AFM.[37] The authors proposed that the two components were miscible at low molar fractions of 10,12-TRCDA and segregated at both higher diacetylene concentrations and high surface pressures. They subsequently examined 10,12-TRCDA/DMPC Langmuir films by BAM and poly(10,12-TRCDA)/DMPC LS films by fluorescence microscopy, and again saw phase separation.[38] Segregation of the PDA and phospholipid domains allows incorporation of cell membrane components, such as membrane proteins, that require lipid stabilization into the phospholipid domains and increases the biomimetic character of the material.

Improving film quality, as shown by increased thermal stability, more uniform surfaces, and larger film areas, has been the subject of several research efforts. A mechanical study of LB films using AFM and contact angle measurements on unpolymerized and polymerized 10,12-PCDA found that polymerized films were more stable to surface rearrangement and deformation than unpolymerized films.[13] Annealing LB films at elevated temperatures prior to polymerization improved crystalline packing by XRD, shifted the absorbance maximum up to 700 nm, and increased the thermochromic reversibility up to 90 °C.[39] A modification of the LS technique using a stream of nitrogen to create turbulence at the air/water interface and a heated substrate resulted in uniform films whose fluorescence varied only 5% over 18 $cm^2$.[40]

An alternate tactic for improving film chromic stability involves increasing the H-bonding of the headgroups. Leblanc and co-workers prepared Langmuir films of a two-tailed diacetylene amphiphile with a triazine headgroup coordinated to a complementary H-bonding small molecule (barbituric or cyanuric acid), which showed greater stability than the classic 10,12-PCDA films in every respect.[41] The films had higher

 

surface pressures at the breaking point, did not convert from blue to red with extended irradiation, had higher onset temperature for blue to red thermal conversion and required much higher temperatures for irreversible chromic conversion. A second study by Leblanc's group further investigated the effect of H-bonding in the headgroups on film stability, but avoided complications from cross-linking by using a series of single-tail diacetylenes with dipeptide headgroups.[42] This series differed only in the amino acid unit closest to the diacetylene tail, with the side chain increasing in size from hydrogen (glycine), to methyl (alanine), to isopropyl (valine), to benzyl (phenylalanine). Increasing side chain size led to increasingly red films upon polymerization. Ahn *et al.* also explored the effect of H-bonding on the stability of PDA LS films to thermal and pH stresses using 10,12-pentacosadiynamides with *ortho*, *meta*, and *para* aminobenzoic acid headgroups (Scheme 4, **7a–c**).[43] LS films of **7b** showed stronger H-bonding *via* FTIR and remarkable thermal and pH stability relative to 10,12-PCDA and the other compounds in the series.

Single-layer Langmuir films have been used for UV-vis detection of bio-analytes though the relatively low levels of PDA present in a monolayer complicates spectroscopic based detection. Geiger *et al.*[32] and Jelinek and co-workers[44] found that at least three diacetylene layers are required for chromic detection. Multi-layer LB and LS films have been used for a variety of detection platforms, as discussed in Section 4, but they are relatively complicated to prepare, require skilled workers and/or sophisticated automation, and it is difficult to create large area films of consistent quality.

*2.2.1.2 SAMs.* Another method of making two-dimensional PDA arrays is by preparation of SAMs from diacetylenes on surfaces and polymerizing them. Most diacetylene SAMs have been formed from thiol monomers on gold surfaces, but the formation and polymerization of diacetylene monolayers on pyrolytic graphite has also been reported.[45] The creation of SAMs from diacetylenic thiols on gold and their subsequent polymerization was first reported in 1994.[46] The SAMs showed some evidence of disorder at the surface based on contact angle measurements, but also showed highly ordered local areas by grazing-angle FTIR. Polymerization was accomplished with 254 nm UV light and Raman spectroscopy showed no additional polymer formation after 30 s. The polymerized coatings were blue, and showed no evidence of conversion to red with continued UV exposure or upon exposure to good solvents for the monomers.

Crooks and co-workers deposited a SAM of diacetylenic thiols with a terminal carboxylate on gold and built up multilayer structures by reaction with additional monomers to form thioester linkages (Scheme 5, **8a**).[47] This layer-by-layer approach in combination with polymerization of the diacetylenes resulted in a 3D network. They subsequently reported preparation of SAMs of different diacetylenic thiols on gold with terminal methyl, hydroxyl, and carboxyl functionality (**8a–c**) and characterized the coatings by SERS, FTIR, UV-vis, and electrochemical methods.[48] The SAMs were photopolymerized and UV-vis spectra acquired; however, the gold substrate probably interfered with the spectral analysis as discussed below. The authors demonstrated that these PDA

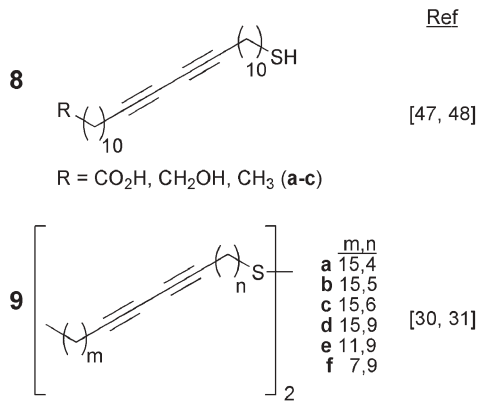


**Scheme 5**

SAMs are much more stable to desorption than traditional alkane SAMs when exposed to electrochemical cycling, increased temperature, and aggressive solvents.[49]

Evans and co-workers performed several careful studies looking at differences between diacetylene monolayers and traditional alkane monolayers on gold (Scheme 5, **9a–f**).[30,31,50] In the first study,[50] they examined the impact of substrate preparation, investigating evaporated, sputtered, and colloidal gold substrates, in order of decreasing flatness. The substrate flatness affected the crystallinity of the diacetylene SAMs and their subsequent polymerization, with higher order and conversion seen on the evaporated gold surfaces. This result was contrasted against the case of *n*-alkyl monolayers, which were not greatly affected by substrate flatness. They note in this publication that UV-vis spectroscopy is not a useful method for characterizing polymerization in PDA SAMs on gold as the broad peak at 650 nm that grows in with UV irradiation, previously ascribed to PDA, also appears when plain alkane thiol monolayers on gold are irradiated with UV light. In the second[31] and third[30] studies they investigated the effect of diacetylene position and the influence of odd and even numbers of methylenes on SAM formation and polymerization as discussed in Section 2.1.1.

SAMs have formed interesting model systems for studying the ordering of diacetylenes on surfaces and the formation of PDA in coatings, but unlike LB films, they have not as yet been shown to have particular sensing applications. The small amount of PDA in the monolayers makes detection of optical signals challenging; however, they might have applications in an evanescent wave fluorescence or plasmon surface resonance detection platform.

*2.2.1.3 Multi-layer coatings.* Casting diacetylenes onto substrates or depositing them onto filters are alternative methods to Langmuir or self-assembled monolayers for preparing extended solid supported arrays of PDA. These methods form multilayer coatings through less controlled processes than either LB films or SAMs; however, they are also faster and more easily scaled. Evaporation of the solvent from organic solutions or aqueous suspensions of acetylenes is the most common approach to generating these thick films on solid supports, relying on self-assembly processes to align the diacetylenes appropriately for polymerization. More recently,

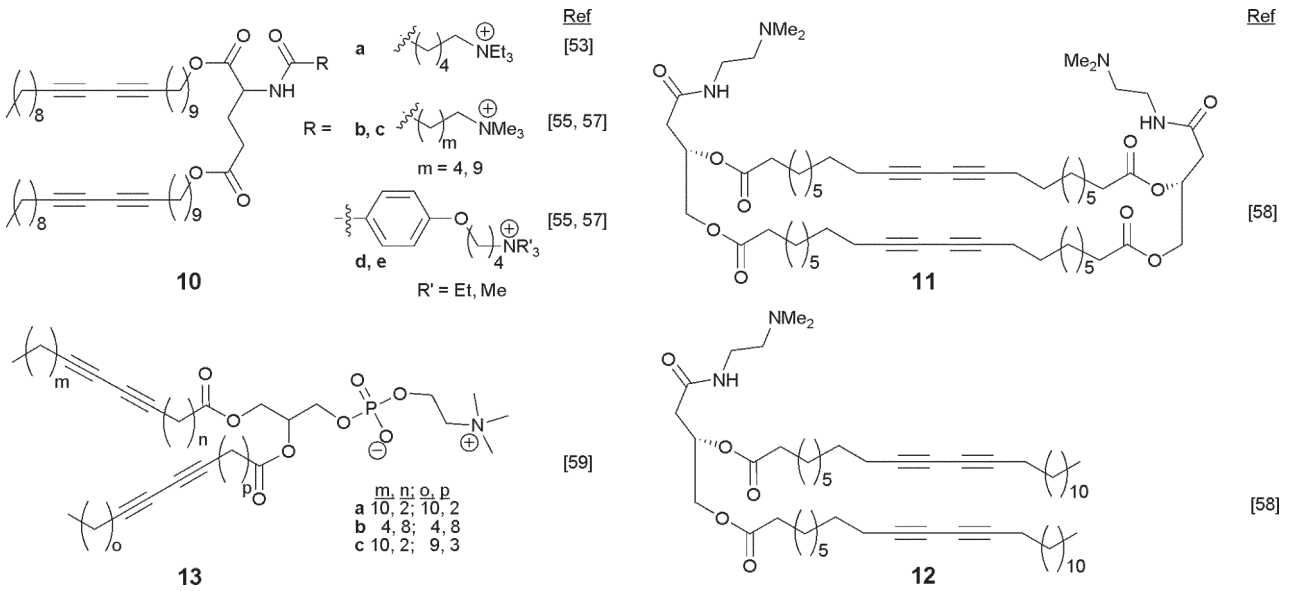


**Scheme 6**

we have developed methods for preparing coatings on nanoporous filter membranes *via* filtration deposition of diacetylene colloid solutions.[51,52]

In a short series of papers, Kuo and O'Brien presented two-tailed ammonium bromide diacetylenic lipids based on a glutamate backbone (Scheme 6, **10a–c**), explored their self-assembly in water and cast them as films on glass.[53–57] The films were polymerized to form blue/purple PDA that was reversibly converted to red at around 50 °C. The polymerized films could be removed from the support as flexible, free-standing films. Wang and Hollingsworth prepared chiral phospholipids analogues with diacetylene chains and amide ethyl dimethylamine headgroup in two variations; one as a bolamphiphile and the other as a monoamphiphile (Scheme 6, **11**, **12**).[58] Films were cast from chloroform and photopolymerized to form blue PDA. The films were extremely flat by AFM and laser scanning confocal microscopy, and XRD showed lamellar packing. Characterization by near-IR spectroscopy showed absorbance maxima above 800 nm, well beyond the usual 600–680 nm of blue PDA. The authors modeled the packing of the phospholipid analogues using MM3 force field calculations and suggested that the diacetylenes pack closely, forming stabilizing π-π interactions, promoting long-range order in the material. Rhodes *et al.* examined the structure of four diacetylenic PC bilayers (Scheme 6, **13a–d**), formed through evaporation of aqueous lipid suspensions, by low angle XRD.[59] All showed a lamellar structure; however, only 1,2-bis(octadeca-4,6-diynoyl)-*sn*-glycero-3-phosphocholine (**13a**) had a well-ordered structure with no chain interdigitation, and polymerized readily. These polymerized bilayer films showed an irreversible thermochromic change around 40 °C. Notably, very little difference in bilayer spacing was seen between blue- and red-form polymer at the same temperature.

We have shown that diacetylene liposomes and other colloids can also be deposited onto nanoporous membranes to form coatings; this technique provides a swift and easy method for forming PDA arrays.[51,60] Coatings were deposited onto both free-standing membranes and onto membranes in 96-well filter plates;[52] photopolymerization of the deposited diacetylenes usually formed blue, non-fluorescent PDA. The liposomes fused to form coatings that range in thickness from 1 to 3 μm with the thickness and morphology dependent on the nature of the diacetylene

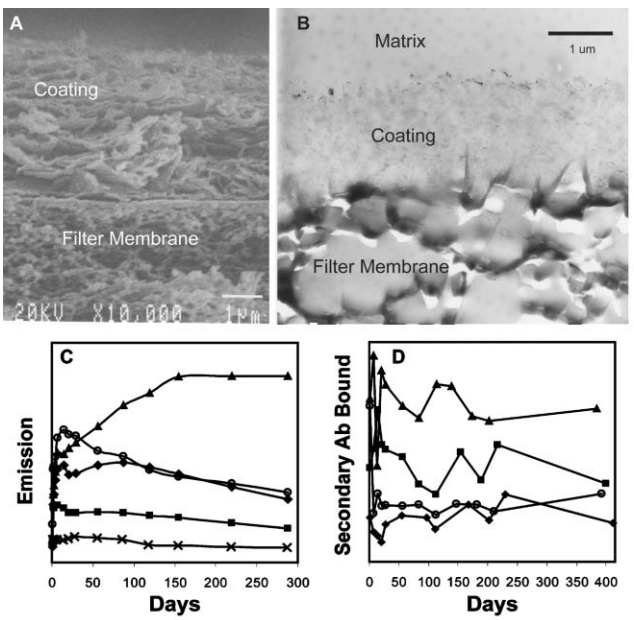


**Fig. 3** Characterization of PDA coatings on nanoporous membranes. (A) SEM of poly(**4**) (Scheme 3), 1 μm scale bar. (B) Immuno-TEM of poly(10,12-PCDA) with surface antibodies labeled with gold clusters, 1 μm scale bar. (C) Emission of poly(10,12-TRCDA) (◆), poly(2-hydroxyethyl 10,12-tricosadiynamide) (■), poly(6,8-DCDA) (▲), poly-(10,12-TRCDA)/DMPC (○), and poly(**2c**) (×) coatings over time. (D) Immunoassays on poly(10,12-PCDA) coatings with antibodies over time. Antibodies were conjugated to different alkyl tails and inserted into liposomes *via* detergent dialysis prior to coating deposition.

 

monomer (Fig. 3(a), (b)). The fluorescence stability of coatings on different membrane types was monitored over a year and the results showed that stability was dependent on both the monomer tail structure, headgroup and the membrane material (Fig. 3(c)).

We also prepared coatings from liposomes with antibodies incorporated by detergent dialysis; the presence of the antibodies in the coatings was confirmed by immunoassays, sandwich assays and by labeling with secondary antibody–gold conjugates and visualization by TEM (Fig. 3(b)).[52] The stability of the antibody presentation was characterized by immunoassay over time and it was seen that the presentation was stable or declined only slowly over the course of more than a year (Fig. 3(d)). Ligands, including antibodies, peptides, aptamers, and phage particles, have also been conjugated directly to the coating surfaces through standard bioconjugation chemistries, such as NHS/amine, maleimide/thiol, and aldehyde/amine couplings.[61]

**2.2.2 Colloids.** Diacetylene amphiphiles can be dispersed in water, usually by probe sonication,[4] to form self-assembled particles, and photopolymerized *in situ*. These colloidal dispersions form alternative PDA materials formats to the films and coatings discussed above, are easier to prepare and more readily scaled to larger volume production. They are also more easily used as reagents in assays than films or coatings as they can be readily dispensed in controlled amounts. A significant disadvantage of these materials, however, is that the PDA particle dispersions may aggregate and/or settle out of solution. Another disadvantage is that post-preparation modification of the colloids, such as conjugating reactive or binding groups to their surfaces, requires size exclusion column chromatography or dialysis steps to separate unreacted material from the liposomes. Neglecting to remove unreacted antibodies or other ligands opens the possibility of competitive binding by the free ligands to targets and reduction of the response of the PDA materials. These disadvantages can be addressed by attaching the polymerized colloids to surfaces. In general, the ease of preparation and biomimetic nature of the PDA colloidal materials have made them a popular platform for developing bioassays.

*2.2.2.1 Liposomes/vesicles.* The formation and polymerization of diacetylene liposomes (or vesicles) followed a few years after the initial work with Langmuir films.[62] The words liposomes and vesicles have been used somewhat interchangeably to refer to spherical particles composed of bilayers (Fig. 2); for simplicity, we will use the term liposomes in this article. The formation of polymerized liposomes, including PDA liposomes, and the advantages and disadvantages of such systems as models for biological membranes, has been discussed in earlier reviews.[8,9,63] Ringsdorf and co-workers noted early on that PDA liposome membranes lacked the fluidity characteristic of biological membranes, though with increased stability to detergents.[64] It is possible to incorporate significant percentages (in our experience up to 70%) of non-polymerizable lipids in diacetylene liposomes to give them a more biomimetic character and still photopolymerize the diacetylene components to form PDA.

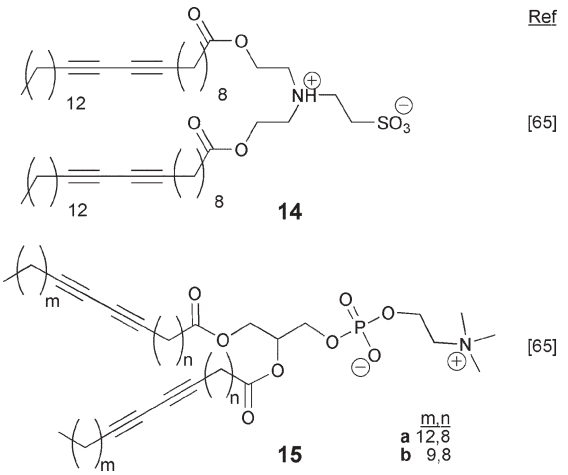


**Scheme 7**

The early work with PDA liposomes focused on creating stable biomimetic membranes using two-tailed diacetylenes[65,66] and phospholipids with diacetylene tails (Scheme 7, **14** and **15a**).[64,67–70] Ringdorf and co-workers also synthesized single-tail diacetylenes with a variety of headgroups similar to those previously used in films,[2] including diacetylenes with phosphate (Scheme 3, **4**),[65] glucose, and lactose headgroups.[71] Bader and Ringsdorf also investigated membrane-spanning diacetylene bolaamphiphiles,[72] synthesizing both symmetric and asymmetric lipids,[73] preparing liposomes and polymerizing them into the blue or red phase. They found that single chain symmetric bolaamphiphiles did not polymerize in liposomes unless cholesterol was added, while asymmetric bolaamphiphiles where the headgroups differed significantly in size formed polymerizable structures.

O'Brien *et al.* have noted that the topochemically constrained two-electron polymerization of PDA can lead to lower polymer yield relative to monomers which polymerize *via* a radical mechanism.[9] O'Brien and coworkers showed that symmetric two-tailed monomers polymerized 6500-fold more efficiently than diacetylene phospholipids, which have non-equivalent tails,[74] presumably because all of the diacetylenes were well aligned for polymerization. A study using a diacetylenic PC (Scheme 7, **15a**) explored the effect of liposome size on polymerization and observed improved polymerization with increasing liposome size,[75] suggesting that if the liposome curvature is too high, the diacetylenes cannot align appropriately for polymerization.

Jelinek and co-workers have studied the poly(10,12-TRCDA)/DMPC liposome system.[76] UV-vis spectroscopy of a series of four polymerized liposomes with 33, 50, 66 and 100% 10,12-TRCDA showed increasing absorbance intensity. DLS and SEC analysis were used to confirm that the liposome composition is mixed. The polymerization of the liposomes, despite the incorporation of significant amounts of DMPC, suggested the formation of separate diacetylene and DMPC domains similar to those seen in film systems.[38] DSC on non-sonicated multilamellar particle suspensions, showed a reduction in enthalpy for the DMPC transition compared to pure DMPC suspensions, but little change in the PDA transition when compared to pure poly(10,12-TRCDA) suspensions.

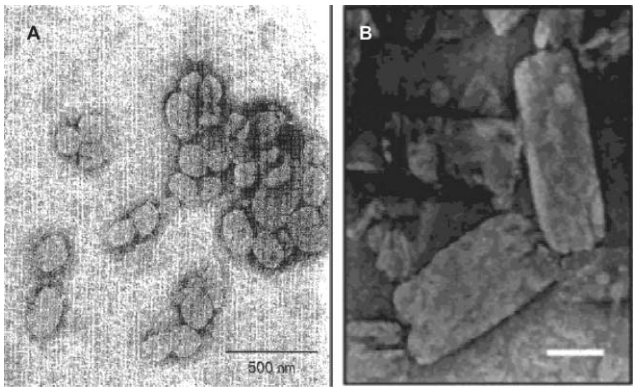


**Fig. 4** TEM images of 60% poly(10,12-TRCDA)/40% DMPC showing (A) liposomes (500 nm scale bar). Reproduced with permission from ref. 77. Copyright 1998, Current Biology Ltd. and (B) sheets (100 nm scale bar). Reproduced with permission from ref. 78. Copyright 2001, Plenum Publishing Corp.

SAXS data, also on multilamellar particle suspensions, showed two broad peaks for poly(10,12-TRCA)/DMPC liposomes, which were assigned as primary diffraction peaks of phase separated poly(10,12-TRCDA) and DMPC. Addition of either DMPG or cholesterol sharpens both sets of peaks, indicating an increase in structural order. ESR using liposomes mixed with 1% spin-labeled stearic acid showed reduced mobility for the labeled lipid with incorporation of cholesterol and hence reduced fluidity. Additionally, liposomes containing cholesterol were more resistant to thermal change than those without. These results taken together paint the somewhat complex picture that the presence of DMPC in the liposome does not affect the enthalpic transitions of the PDA while the order of the DMPC does affect the PDA chromic stability.

Interestingly, TEMs of 60% poly(10,12-TRCDA)/40% DMPC particles published in different papers vary. Jelinek, Charych and co-workers published images of spherical (or semi-spherical) vesicles in 1998,[77] while Jelinek and co-workers in later work presented TEMs of the particles that showed them as sheets rather than vesicles (Fig. 4).[78] Jiang and co-workers subsequently published TEMs comparing poly(10,12-TRCDA) and 60% poly(10,12-TRCDA)/40% DMPC particles conjugated to antibodies.[79] The TEMs showed that poly-(10,12-TRCDA)-antibody with no DMPC forms vesicles, whereas 60% poly(10,12-TRCDA)/40% DMPC-antibody forms flat sheets. These variations in self-assembled structure observed for the same formulation suggests that either (i) intrinsic variability in the liposome preparation method affects structure, (ii) the as-formed structures are not stable over time, or (iii) the variation is an artifact of sample preparation for TEM. As a further example, we have recently prepared and thermally converted 60% poly(10,12-TRCDA)/40% DMPC formulations in water and in 2 mM HEPES at pH 7.4 and saw by fluorescent microscopy that the formulation forms liposomes in water and fibers in HEPES buffer. These examples highlight the importance of preparation conditions, an area that is often neglected in experimental details.

*2.2.2.2 Non-spherical colloids.* A number of diacetylene lipids have also been discovered that self-assemble into a variety of non-spherical structures such as tubules,[80–82] helices, ribbons, and sheets.[83–85] The early work with diacetylene lipid tubules was performed with diacetylenic PCs, most commonly bis-(10,12-TRCDA)-*sn*-glycero-3-phosphocholine (Scheme 7, **15b**), and has been previously reviewed with discussion covering synthesis, tubule formation, IR and Raman spectroscopy and electron microscopy.[80] Subsequent work has been performed studying the formation of tubules from **15b** liposomes,[81] and using asymmetric diacetylene bolaamphiphiles to form fibers, ribbons and sheets.[86–88] A recent review discusses formation of PDA nanowires from strongly H-bonding symmetric bolaamphiphiles, and from asymmetric bolaamphiphiles with one head group capable of π–π stacking and the other H-bonding.[11]

Initially, all of the monomers that were known to form non-spherical colloids were chiral and it was believed that the molecular chirality was the basis of structural chirality (*i.e.* helices and helical twists observed in tubules).[89] An achiral isomer of **15b** (Scheme 8, **16**) was subsequently prepared and used to demonstrate that molecular chirality is not necessary for the generation of chiral tubules.[90] The achiral molecules still formed helical tubules, as a racemic mixture of left- and right-handed tubules. More recently, tubules were formed from the hydrobromide salt of a single chain achiral diacetylene amine in water (Scheme 8, **17**).[91] These tubules were observed to be monodisperse and have a distinct CD spectrum, despite lacking any chirality in the monomer. The authors hypothesize that interaction between the bromide counter ion and one of the hydrogen atoms on the ammonium headgroup creates an effective chirality, leading to the generation of chiral microstructures. When these tubules were deposited on a surface and polymerized, a regular array of tubules were formed normal to the surface. The polymerized tubules were blue and showed increased resistance to temperature and solvents.[92]

Tubules, ribbons and fiber structures form an interesting contrast to liposomes. For example, Plant *et al.* showed that **15b** was more tightly packed in tubules than liposomes.[81] These non-spherical structures generally have significantly larger dimensions than liposomes, many examples have lengths greater than 10 μm. The structures are often not stable in solution, forming gels and aggregates. While the PDA in these structures has shown similar chromic behavior to PDA liposomes in response to heating and pH changes,[85,88] they have not, to date, been explicitly used in biosensing

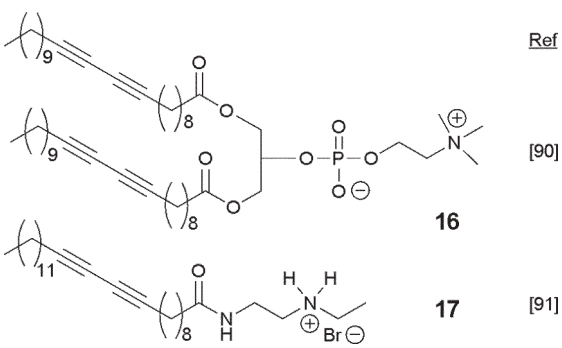


**Scheme 8**

applications. It should be noted, though, that given the variability in particle structure discussed above that in some cases where reports indicate that liposomes are used, but the particle shape is not characterized, other structures may be present or even dominate.

One potential disadvantage of liposomes and other colloids are their tendency to aggregate and fall out of solution. We have studied the effect of adding divalent and monovalent cation salts to poly(10,12-PCDA), poly(6,8-DCDA) and poly(10,12-P-EtOH) liposomes prepared in deionized water and determined that all of the liposome formulations aggregate swiftly when exposed to $MgCl_2$, $MnCl_2$, and $CaCl_2$ at concentrations greater than 1 mM and more slowly at lower concentrations.[93] The liposomes were more stable to monovalent cations; however, they still aggregated in 200 mM NaCl and KCl solutions after an hour. The fatty acid liposomes also aggregated in 1% BSA. As many bioassays require the presence of salts and proteins, we have moved to attaching our liposomes to surfaces to avoid these problems.

**2.2.3 Immobilized liposomes.** Liposomes can be immobilized to prepare another category of PDA materials. Immobilization has been achieved through encapsulation, physical adsorption, non-covalent bonding, or covalent reaction; immobilization allows the use of liposome structures under conditions where aggregation is usually a problem (*e.g.* with divalent cations or at high protein concentrations).

Sasaki and co-workers demonstrated encapsulation of PDA liposomes by preparing poly(5,7-DCDA) liposomes and trapping them in a silica sol–gel.[94] The encapsulated liposomes remained purple after entrapment and could be converted to red by heating to 55 °C. Gill and Ballesteros also encapsulated PDA liposomes in sol–gel matrices.[95] In this case mixed liposomes, fatty acid aminoethylamides with phospholipids, were modified with antibodies and then encapsulated in organic/inorganic hybrid sol–gels. The authors reported that these materials were rugged and easily processed, and that the encapsulated liposomes remained accessible to soluble proteins.

Jelinek and co-workers have recently described preliminary work on immobilization of PDA in agar for bacterial detection.[96] Unpolymerized mixed liposomes of 60/40 10,12-TRCDA/DMPC were mixed with hot Luria–Burtani agar and allowed to cool. The TRCDA in the composite material was polymerized with UV light and formed blue PDA; bacterial growth on the agar caused the PDA to turn red.

PDA liposomes have also been attached to surfaces. Singh and co-workers immobilized polymerized PDA liposomes on a gold surface using liposomes containing disulfides, and characterized the surface using AFM, reporting robust monolayer coverage.[97] Ahn and co-workers immobilized liposomes of an amine terminated 10,12-PCDA on aldehyde modified glass slides by Schiff base formation.[98] The liposomes could be polymerized before or after immobilization, but if they were polymerized first they converted to red when immobilized. If they were immobilized first and then polymerized they were blue. SEM was used to demonstrate that the liposomes did not open up when attached to the surface. Additional immobilization work was performed with 10,12-PCDA liposomes attached to micro-contact printed amines surfaces.[99] These liposomes initially contained activated 10,12-PCDA NHS esters, but the liposome preparation involved probe sonication and heating in water to 80 °C, which could hydrolyze the NHS esters. So it seems possible that this preparation resulted in non-covalent, H-bonding between the liposome carboxylic acids and the surface amines. Again, if the liposomes were polymerized before immobilization they converted upon attachment to the surface, but not if they were immobilized and then polymerized. Fluorescence microscopy images of converted liposomes demonstrated exclusive attachment to patterned areas of the glass. Ahn and co-workers subsequently showed that immobilized liposomes, attached through Schiff base formation, could be patterned by polymerization through a mask and by deposition with a standard microarray spotter.[100]

We have attached PDA liposomes to microporous glass filters modified with surface epoxides using chemical reactions between thiols (usually DPPT) incorporated in the liposomes and the epoxides on the glass.[101] The immobilized liposomes can be polymerized into the blue form. Cryogenic TEM of mixed PDA/phospholipid attached liposomes confirm that they do not open up on the glass surface, but remain individual liposomes (Fig. 5). Immobilization reduced the liposome response to buffers, including to those containing divalent cations. We have shown that immobilized liposomes can be used in bioassay applications, as discussed in Section 4.

**2.2.4 Material forms conclusion.** PDA can be generated in a wide variety of self-assembled structures as long as the diacetylene monomers are organized in the correct geometry for the topochemical polymerization. PDA Langmuir films and liposomes have been studied extensively since the inception of the field; more recently new material formats such as SAMs, multilayer coatings and immobilized liposomes have been prepared. Specific material forms offer specific advantages for different biosensing applications. For example, colloidal solutions are suitable for assay applications where liquid handling techniques are used, such as automated high throughput screening in drug discovery. In contrast, solid supported PDA materials are more suitable for incorporation in devices where ruggedness and ease-of-use are paramount design considerations. The variety of PDA structures has also

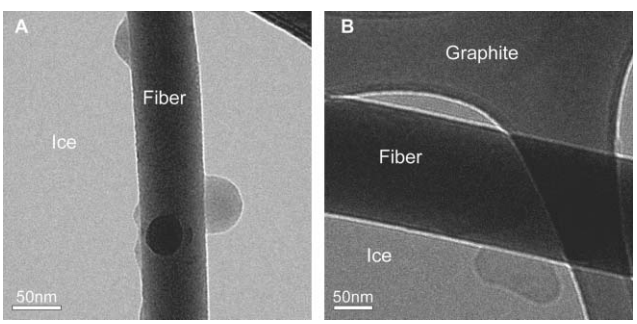


**Fig. 5** Cryogenic TEM images of PDA liposomes attached to glass fibers.

provided platforms for studying the exciting material and optical properties of this unique polymer.

## 3 Optical properties

The optical properties of PDA materials arise from the π-conjugated polymer backbone. The non-linear optical and electronic properties of PDA first excited interest in the PDA materials;[102] however, the vast majority of work on developing PDA sensing materials has focused on their environmentally sensitive chromic properties, with more recent work taking advantage of the emissive properties.

### 3.1 Color

Absorption spectra of PDA materials typically contain several peaks with maxima at *ca*. 650, 550 and 500 nm (Fig. 1(a)). These peaks are associated with the blue (650 nm) and red forms of PDA (550 and 500 nm). A peak at *ca*. 600 nm appears as a shoulder to the 650 nm peak. This peak has been attributed to a "purple" form of PDA,[4,41] postulated as an intermediate between the red and blue forms.[103–105] It should be noted that this proposed "purple" form is distinct from the purple color seen when there is a mixture of blue and red forms. An absorbance peak at 450 nm has also been reported for a green PDA solid[17] and a peak at *ca.* 440 nm for yellow solutions of PDA chains.[106,107] Absorbance peaks at 704 nm,[27] 717 nm,[108] 818 nm and 848 nm,[58] have also been observed for PDA films and particles; these are rare but are correlated with exceptionally stable materials. The appearance and ratio of absorbance peaks for given PDA material depend on the structure of the polymer side chains, the extent of polymerization, the polymer's material form (dilute solution, film, liposome, *etc*.), and the environment of the polymer (temperature, pH, solvent *etc*.). Color change has been observed for PDA materials upon heating, solvent changes, exposure to vapors,[109,110] and changes in pH, usually with reduction of higher wavelength absorbances and growth of lower wavelength absorbances. These changes register to the eye as shifts from blue to red, red to yellow *etc*. Chromic changes of PDA materials in response to environmental stimuli have been the basis for the majority of PDA-based detection systems.[4]

**3.1.1 Mechanisms of color and emission change.** Considerable research effort has been devoted to elucidating the mechanisms of color and emission change in PDA materials caused by environmental changes. This has proven to be a difficult challenge and the mechanisms are still not fully understood. The issue is complicated by the likelihood of multiple mechanisms causing chromic change, with the specific mechanism dependent on the nature of the environmental stimulus. Studies have shown that both side chain order and headgroup H-bonding affect the chromic state and the susceptibility to chromic change of PDA materials. Imperfect communication and understanding between different subfields, particularly the physics and chemical/material science fields, further confuses discussion of the interplay between the optical/electronic nature of the conjugated polymer backbone and the ensemble material structure.

*3.1.1.1 Theoretical and single chain studies.* The electronic basis for the different color forms of PDA has been examined theoretically and also through studies of isolated chains. At the simplest level, the PDA chain has been modeled as a particle-in-a-box system;[111] the different absorbance peaks represent different conjugation lengths of the π-bonds of the polymer backbone with termination of the lengths either by twisting of the backbone to break the conjugation or by reaching the end of the polymer.[17] More sophisticated theoretical studies have been performed to predict the absorbance characteristics of PDA,[25,112] and the effect of conformational changes of the backbone on the PDA color.[26,113]

Soluble PDAs with alkoxy carbonyl methylurethane side chains (nBCMU, where n is the number of carbons in the alkoxy group) form simple and well-studied systems that were first used to understand PDA chromic changes. These chains have been examined in good and bad solvents using absorption, emission, infrared and Raman spectroscopy, dynamic light scattering, small angle X-ray and neutron scattering, and nuclear magnetic resonance; these studies were reviewed by Chu and Xu.[106] The general conclusion is that the color and emission of the chains is dependent on the aggregation state; in poor solvents (for example, toluene) the chains form extended rod structures with longer conjugation lengths and a red color, they also aggregate over time. In good solvents (for example, chloroform) or at higher temperatures the chains form discrete coils of varying size dissolved as a yellow solution. The solutions can be converted from one color to the other by solvent addition or temperature changes. These changes parallel the changes seen in films and liposomes, where the color shifts are more commonly from blue to red, rather than red to yellow.

Single PDA chains have been formed and studied at low temperatures in diacetylene crystals as an experimental model for investigating the electronic state of the PDA backbone.[114–119] These studies have been summarized by Schott, who in a recent commentary, argues that as the exciton formed in the isolated red chain is spatially coherent along the whole chain length of $\sim$20 μm, "conjugation length" is not a relevant concept for explaining color transitions in PDA.[119] He points out that as long as the conjugation length is larger than the exciton Bohr radius ($\sim$2 nm) the conjugation length will not affect the exciton energy. Schott proposes that the difference between red and blue PDA is the result of different chain geometries. The repeat units in the red chains are rotated relative to the average plane, and have smaller transfer integrals, while the blue chains are planar. He also argues that the change from blue to red should be regarded as a phase change involving the whole system. The abandonment of the conjugation length concept is consistent with Dobrosavljevic and Stratt's earlier theoretical work;[26] however, changes in conjugation length are still invoked by material scientists working with PDA to explain color changes.[7] Furthermore, while the isolated chain model systems allow examination of the electronic states of the PDA backbones in the blue and red forms, they do not include the electronic interactions between backbones that are a factor in other conjugated polymer materials.[10,120]

 

*3.1.1.2 Film and liposome chromic studies.* Many studies have been performed on PDA films and liposomes investigating chromic change caused by temperature changes,[7,41,85,121–124] pH shifts,[85,125–128] and UV exposure,[7,41] characterizing the structure of the materials in the different color phases. Early studies using IR[121] and DSC[129] supported the hypothesis that the color change was caused by changes in the packing of the polymer side chains. Electron diffraction[130] and AFM experiments[123,124] showed that both blue and red PDA films were ordered, though with different lattice geometries.

We have found three examples where the bilayer spacing of blue phase and red phase PDA were compared, and three different behaviors observed. First, Rhodes *et al.* observed very little difference between blue and red phase PC PDA films by XRD.[59] Second, Charych and co-workers saw a 15% increase in bilayer spacing by AFM when poly(10,12-PCDA) films were converted thermally.[124] And finally, Burns and co-workers observed a decrease in height by AFM when blue-phase PCDA and P-EtOH films were converted mechanically.[7] These different results in spacing change upon conversion suggest that there are multiple mechanisms leading to conversion and that those mechanisms depend on both the material composition and the method of initiating conversion.

FTIR studies of PDA materials undergoing pH induced chromic shifts show that the colorimetric change is correlated with changes in headgroup H-bonding and geometry.[85,125–128] As discussed in Section 2.2.1.1, LeBlanc and co-workers demonstrated that extensive H-bonding made PDA films resistant to chromic changes caused by temperature and UV light.[41] Subsequently, Cheng and co-workers showed that during thermochromic changes the H-bonding of amino-acid headgroups remained unperturbed, while under deprotonation conditions the H-bonding was reduced.[85]

Recently, results published by Kew and Hall showed that the effect of deprotonation on the absorbance of PDA carboxylic acid based liposomes is dependent on the cation present and the extent of the PDA response to base can be amplified or attenuated by the presence of different cationic species.[128] The authors hypothesize that there is a multi-step mechanism for color change consisting of deprotonation of the headgroup, cation binding to the headgroup, and rearrangement of the headgroups. The rearrangement of the headgroups changes the packing of the methylene side chains as shown by IR.

PDA films have also undergone chromic shifts induced by mechanical stress.[7] Burns and co-workers used mono- and trilayer PDA films to examine mechanochromism with scanning near field microscopy (SNOM), AFM, and ellipsometry.[104,131,132] They propose that blue-phase PDA is metastable, as polymerization of diacetylenes without reorganization of the side chains results in the formation of stress in the material. Conditions that provide enough energy to overcome side chain packing, such as mechanical force, heat and extended polymerization, permit the backbone to reorganize to relieve that stress, turning it red.

Burns and co-workers also observed conversion from blue to red PDA in their films at temperatures consistent with 10,12-PCDA in other forms.[34,103,124] At elevated temperatures, however, the authors observed a shift in maximal absorbance wavelength from 640 nm to 600 nm; they assigned the 600 nm peak to a ''purple'' phase (or form). This shift is only observed when a blue phase sample is heated; heating red-phase films does not generate the 'purple' phase and cooling from the 'purple' phase gives predominantly blue-phase material.

*3.1.1.3 Mechanisms of chromic change.* It can be seen from these studies that the understanding of color change in PDA materials, formed from assemblies of PDA backbones with side-chains and affected by changes in the packing of the side chains and H-bonding in the headgroups, has evolved as different groups have studied the packing, bonding and colors of PDA materials. Rotation of the single bonds in a theoretical PDA backbone without side chains is predicted to cost little energy and be thermally accessible at room temperature; however, such rotations in real PDA materials involve changes in the packing and inter-chain interactions of side-chains.[26] Conformational changes in the polymer backbone, and changes in the structure of the side chains assembly, including both the packing of the methylenes and bonding interactions at the side chain termini (*i.e.*, headgroups), are thus inextricably linked.

Polymerization changes the hybridization of the terminal alkyne carbons from sp to $sp^2$ and therefore changes the preferred bond angle from 180° to 120°, but the packing of the side chains does not allow the polymer backbone to reorient and relieve strain, resulting in accumulation of stress in the material as polymerization proceeds.[7,26] The different routes to chromic change can be thought of as overcoming the barrier to reorganization of the polymer backbone created by the packing of the side chains: higher temperatures increase motion of the side chains and allow changes in the packing of the chains, UV exposure extends polymer lengths and increases the overall stress of the system effectively reducing the energy required for backbone reorientation, and pH changes alter the H-bonding in headgroups allowing the methylenes between the headgroup and the backbone to reorganize. In addition to these enthalpic considerations, transition of the polymer backbone from extended rod like segments associated with the blue form to zigzags[41] or coils[26] proposed for the red form would have entropic gains.

The question of whether the mechanisms for color change caused by biological interactions at the surface of PDA materials, such as analytes binding to targets, interactions with membrane inserting proteins, and enzymatic cleavage of substrates are different from the mechanisms caused by simple environmental influences is still open. It has been generally hypothesized that interactions with biological targets can cause changes in the headgroup H-bonding and alkyl chain packing, similar to those shown for thermochromic and pH based changes,[133] presumably permitting relief of backbone strain as described above. It can be expected, however, that the binding of microorganism at the surface of PDA materials will affect the structure and optical properties of the polymer through different mechanisms than the insertion of a protein into the lipid bi-layer or the cleavage of lipids by an enzyme. Understanding the basis of the optical changes of PDA materials under different conditions is vital to the design of sensitive and stable sensing materials.

### 3.2 Emission

The emissive behavior of PDA materials parallels the chromic behavior: red and yellow PDA are fluorescent while blue PDA is not. The non-emissive nature of blue PDA was observed early on.[111] Blue PDA with urethane side-groups has been studied by femtosecond spectroscopy[134,135] and the quantum yield of blue PDA estimated at $<10^{-5}$, attributed to ultra-fast relaxation of the excited state. The quantum yield of isolated red PDA chains at 15 K was measured at 0.3;[115] whereas the quantum yield of a red PDA film at room temperature was estimated at 0.02.[136] The lower quantum yield of the film can be attributed to the higher measurement temperature as well as potential quenching of the excited state through inter-chain energy transfer. Burns and co-workers noted that the emission of red PDA films decreased with increasing temperature and attributed this to thermal fluctuations of the side chains leading to more non-radiative decay pathways.[104]

Fluorescent (*e.g.*, red) PDA films and liposomes can be excited with wavelengths above 450 nm and emit two broad fluorescent peaks at *ca.* 560 nm and 640 nm.[136] The relative heights of the peaks can vary considerably with some materials showing only the 560 nm peak and others having more intense emission at 640 nm than at 560 nm; the ratio of the peaks is also dependent on the extent of polymerization.[137] Fig. 6(a) shows the example of emission of different PDA fatty acid liposomes with varying tail lengths and distances between the polymer backbone and the headgroups. Fig. 6(b) shows the emission of poly(10,12-PCDA) liposomes polymerized with increasing UV dose and converted to the emissive form by heat; the 640 nm peak gains in relative intensity as the amount of polymer increases. This apparent dependence on polymer concentration supports our hypothesis that the 640 nm emission arises from inter-chain energy transfer prior to emission. While changes in absorbance and emission parallel each other, the emission changes are relatively larger. This can be seen by comparing the absorbance and emissive curves of blue and red PDA liposomes (Fig. 7(a)) and the changes in absorbance *vs.* emission over time (Fig. 7(b)).

We have shown that the emissive profile of PDA materials can also be altered through addition of small molecule fluorophores (Scheme 9, **18** and **19**) that can accept energy from the PDA and emit; this process can also increase the

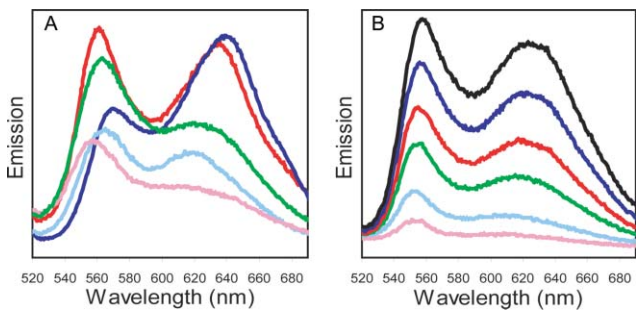


**Fig. 6** Emission spectra of PDA liposomes. (A) poly(10,12-PCDA) (red), poly(6,8-PCDA) (pink), poly(5,7-TCDA) (green), poly(10,12-TRCDA) (blue), poly(5,7-DCDA) (light blue). (B) poly(10,12-PCDA) liposomes exposed to 0.1 (pink), 0.2 (light blue), 0.4 (green), 0.6 (red), 0.8 (blue), 1.0 (black) J $cm^{-2}$ UV light.

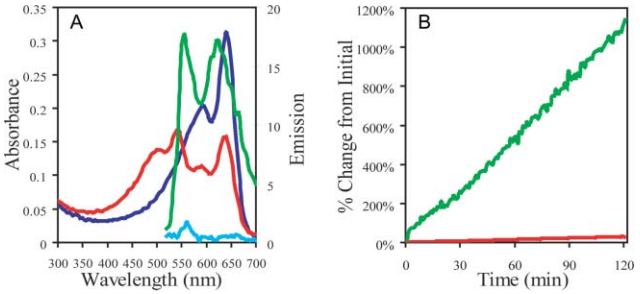


**Fig. 7** Absorbance and emission of poly(10,12-PCDA) liposomes diluted 1:9 with 25 μM $NaHCO_3$. (A) Spectra of absorbance before exposure to base (blue), absorbance after exposure to base (red), emission before exposure to base (light blue) and emission after base (green). (B) Kinetic plot showing change in emission at 560 nm (green) and CR (red) during base exposure.

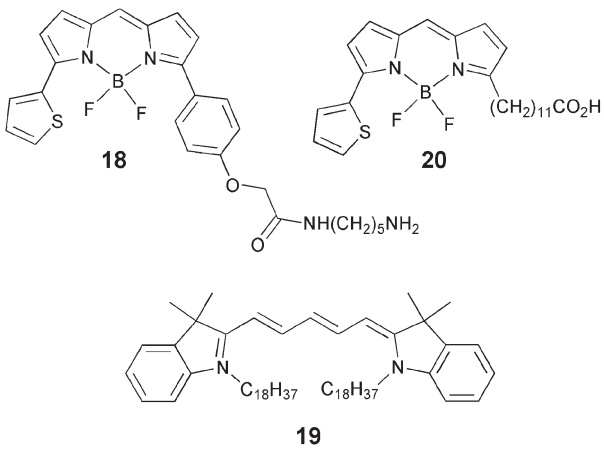


**Scheme 9**

overall quantum yield of the system (Fig. 8).[51,137] The 475 nm excitation wavelength used to excite the PDA does not directly excite the fluorophores to any significant extent. Similarly, PDA excitation can be manipulated through addition of absorbing species that transfer energy to the PDA; this is less useful than the first process, though it also can be used to

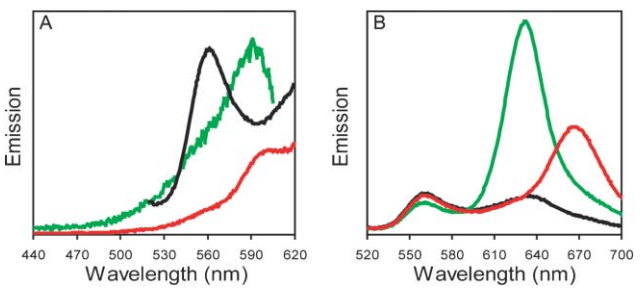


**Fig. 8** Energy transfer from fluorescent poly(10,12-PCDA) liposomes to fluorophores. (A) Comparison of excitation spectra of 5-(((4-(4,4-difluoro-5-(2-thienyl)-4-bora-3a,4a-diaza-*s*-indacene-3-yl)phenoxy)-acetyl)amino)pentylamine hydrochloride (**18**, green) and 1,1′-dioctadecyl-3,3,3′,3′-tetramethylindodicarbocyanine (**19**, red) and the emission spectra of PDA (black). (B) Emission of fluorescent poly(10,12-PCDA) liposomes without fluorophores (black), with 0.5% **18** (green) and with 0.5% **19** (red).

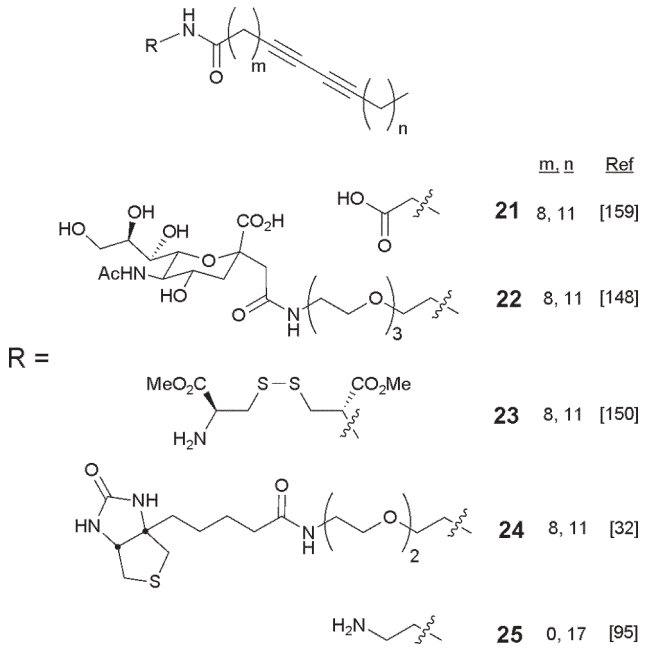


**Scheme 10**

increase the Stokes shift by moving the excitation wavelength into the blue. For example, we have conjugated quantum dots with emission at 490 nm to PDA liposomes and have seen emission from PDA upon excitation of the quantum dots at 400 nm, a wavelength that does not excite PDA significantly.[138] PDA has also been used to quench fluorophores; recent work from Cheng and co-workers presented reversible quenching of 4,4-difluoro-5-(2-thienyl)-4-bora-3a,4a-diaza-*s*-indacene-3-dodecanoic acid (Scheme 9, **20**) incorporated in PDA liposomes prepared from the glycine derivative of 10,12-PCDA (Scheme 10, **21**) upon exposure to amines.[139]

### 3.3 Optical properties conclusion

The optical properties of PDA and their environmental susceptibility form the basis for signal generation in PDA biosensing materials. A picture of the causes of optical change continues to emerge, and how these changes occur in biological detection remains to be determined. Colorimetric detection has been the preferred approach for many years though the emissive properties of PDA have the potential to provide more detection sensitivity. The use of PDA emission for signal generation also allows a wider variety of support materials because they do not have to be transparent. Finally it is possible to amplify the emission signal through energy transfer to incorporated fluorophores, though additional work is needed to fully characterize the process.

## 4 PDA in bio-detection applications

The optical properties, absorbance and emission, of PDA materials are environmentally sensitive, responding to changes in temperature, solvent, and pH, as discussed above. For the first decade after the development of PDA liposomes, they were primarily used as stabilized biomimetic materials for studying proteins,[63,66,140–143] without use of the optical properties for sensing. Charych *et al*. first reported in 1993 that PDA liposomes and films incorporating 10,12-PCDA tails with sialic acid headgroups developed for the inhibition of influenza, changed from blue to red on exposure to the virus.[133,144] Subsequently, they and others have reported PDA liposomes and films with ligands and substrates for the optical detection of small molecules, enzymes, toxins, antibodies, and bacteria. The electronic properties of PDA have also been used for detection;[6,145] however most bio-detection with PDA materials have used the optical properties of the polymer.

The use of PDA materials for sensing has been complicated by the ability of the materials to respond non-specifically to environmental changes, such as buffer ions, osmotic strength and pH. In addition, to the best of our knowledge, there has been no demonstration of reversible PDA response to biological analytes. Reversibility is a very attractive characteristic in sensing materials as it is necessary for a reusable or continuous sensor, themselves highly desirable for environmental sensing applications. The absence of reversible responses to biological targets is not surprising, though, given the generally irreversible nature of chromic changes caused by heat, pH and UV in many PDA materials. The reversible response shown by some materials to pH[127,139] and large temperature changes,[39] suggests, however, that there is potential for the design of reversible PDA biosensors. While it seems unrealistic to expect that detection of bioanalytes strongly affecting the morphology of the PDA materials would be reversible, it is possible that, with appropriate design of the PDA head groups, optical changes occurring from less disruptive binding interactions could be reversed upon release of the target. The many advantages of PDA, including the integrated signal transduction element, biomimetic self-assembly, and the potential for ''reagentless'' detection have driven the development of biosensing materials from PDA.

The detection signal of choice for PDA sensors and assays for most research groups has been the ''colorimetric response'' (CR) of PDA liposomes and films.[4] The CR reports the relative changes in ratio of the blue form PDA and red form PDA in the sensing material over time. An absorbance peak in the range of 650–620 nm is selected to represent the blue form and a second absorbance peak, usually 550 nm or $\sim$500 nm, is selected to represent the red form. The precise choice of wavelengths is dictated by the absorbance maxima of the specific PDA material. As an example, the percentage of blue form can be calculated for each time point (%B($t$)) from the absorbances at 650 nm ($Abs_{650}$) and 500 nm ($Abs_{500}$), and compared to the initial percentage of blue form (%B(0)) to calculate the CR:

$$\%B(t) = Abs_{650}(t)/[Abs_{650}(t) + Abs_{500}(t)]$$

$$CR = \{[\%B(0) - \%B(t)]/\%B(0)\} \times 100$$

An advantage of using the CR for detection is that any systematic effects that affect both absorbances equally, such as aggregation of liposomes out of solution, will not affect the overall detection. When the absorbance signal is weak, though, small changes are magnified by the CR calculation; this can

amplify background effects from non-specific environmental changes and instrument noise.

The emission properties of PDA have been used for analyte detection to a much lesser extent. Fluorescent PDA film sensors for proteins were proposed by Ribi and co-workers using the emission of red PDA films for signal generation in ELISA assays.[146] Ribi also noted the potential for using PDA chromism and emission for detecting protein binding.[5] We have pioneered the use of the changeable emissive properties of PDA coatings and liposomes in combination with energy transfer to fluorophores for detection of enzymatic action[101,137] and microorganisms.[52] More recently, Jelinek and co-workers used PDA emission to detect catecholamines binding to synthetic receptors incorporated in PDA/phospholipid liposomes.[147] Similarly, Ahn and co-workers detected fluorescent changes in immobilized PDA liposomes exposed to α-cyclodextran and poly(acrylic acid).[100] Using emission rather than absorbance for detection has two major advantages: increased system sensitivity as changes in emission are greater than the comparable changes in absorbance, and emission measurements can be made on PDA materials supported on opaque substrates.

### 4.1 Detection of viruses and microorganisms

The genesis of the PDA colorimetric biosensing field was the discovery of Charych and co-workers that LB films[133] and liposomes[148] prepared from 10,12-PCDA and sialic acid terminated 10,12-PCDA (Scheme 10, **22**) changed color from blue to red when exposed to the influenza virus. The virus binds to the sialic acid headgroups *via* hemaglutinin at the virus surface.[149] Both the films and liposomes showed a dose response to influenza virus (Fig. 9). Competitive inhibition of the virus binding to the sialic acid by α-methyl-*N*-acetyl neuraminic acid was measured for the LB films and agreed with literature values; this suggested the utility of this system

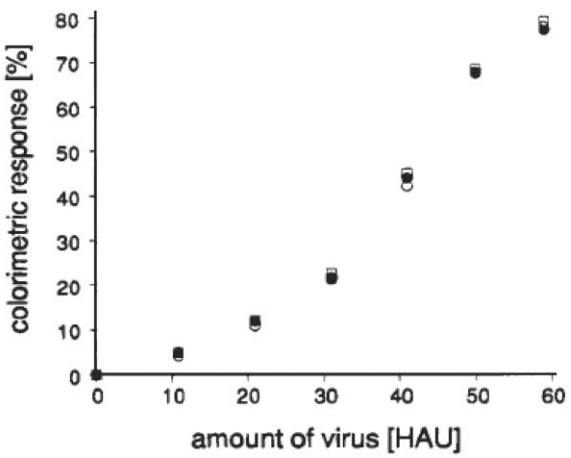


**Fig. 9** Plot of the colorimetric response of a purple liposome solution (5% **22**, 24 min UV) *vs.* successive additions of influenza virus. The liposomes were incubated for 30 min following each addition of virus, and the visible absorption spectrum was recorded. The CR for each virus concentration was obtained in three independent experiments. Reproduced with permission from ref. 148, Copyright 1995, American Chemical Society.

for measuring inhibition activity.[133] Song *et al.* later demonstrated that a more synthetically accessible sulfur linked sialic acid functionalized 10,12-PCDA could be used in lieu of the carbon linked 10,12-PCDA-SA without loss of detection sensitivity.[150]

Detection of bacterial species using PDA materials functionalized with sugars and antibodies has focused on *Escherichia coli*. *E. coli* are a convenient model target as the bacteria are readily accessible and have multiple known ligands that bind to them. Additional interest in detection of pathogenic *E. coli* also provided impetus for these studies. Jiang and co-workers detected *E. coli* with glucoside decorated PDA liposomes.[151] The authors prepared liposomes from 2,4-TRCDA and 10,12-PCDA with 2% dioctadecyl glycerylether-β-glucoside (DGG) incorporated, and exposed them to $\sim 1 \times 10^7$ *E. coli*/mL. The 2,4-TRCDA/DGG liposomes rapidly turned from blue to red, while the 10,12-PCDA/DGG liposomes remained blue. 2,4-TRCDA liposomes without DGG also did not change color when exposed to *E. coli*. In subsequent work, Jiang and co-workers explored the effect of varying the oligo(ethyleneglycol) spacer length between β-D-glucopyranoside and a cholesterol anchor incorporated in 2,4-TRCDA and 2,4-HCDA liposomes on detection of *E. coli*.[152] The authors were able to incorporate up to 10% of the sugar derivative in the liposomes and still photopolymerize the diacetylenes; addition of the derivative at more than 10% significantly reduced the polymerization. The response to $\sim 10^7$ *E. coli* of 2,4-HCDA and 2,4-TCDA liposomes were similar, however, the TCDA liposomes saturated at $\sim 2 \times 10^8$ *E. coli*, while the HCDA response continued to increase up to $\sim 6 \times 10^8$ organisms. The linker length also affected the response of the liposomes: the colorimetric response from material with a 4-unit ethylene glycol linker was greater than the response from a 3-unit linker, which in turn was greater than the response from material with a 1-unit linker.

Li and co-workers reported colorimetric detection of *E. coli* using poly(10,12-PCDA) liposomes with 5% mannoside conjugated to a hexadecane tail incorporated.[153] The liposomes showed a dose response to *E. coli* between $2 \times 10^8$ and $7 \times 10^8$ organisms. The *E. coli* were also pre-mixed with $TiO_2$ colloids as a photocatalyst and irradiated to kill the *E. coli*. The treated *E. coli* caused smaller color change in the liposomes; the longer the time of irradiation (and hence sterilization) of the *E. coli* solutions, the less color change seen upon addition to the PDA liposomes. These results suggest that their detection system is specific to viable *E. coli*.

Supported PDA systems have also been used for *E. coli* detection. Li and co-workers reported preparation of poly(10,12-PCDA) monolayers with 5% 10,12-PCDA tethered to α-D-mannopyranoside *via* a 3-unit ethylene glycol linker (Scheme 4, **6**).[154] The monolayers were deposited onto glass slides and immersed in $CdCl_2$ solutions. The treated slides were then exposed to $H_2S$ to form CdS nano-crystallites at the polymer surface. The UV-vis spectra of monolayers with and without the CdS were very similar. This modification, however, enhanced the CR of the monolayers, from 11% for the unmodified monolayers to 26%, upon exposure to $9 \times 10^8$/mL *E. coli*. The authors propose that the addition of the

 

monocrystallites altered the surface charge of the monolayers from negative to positive, leading to an electrostatic attraction between the bacteria and the surface, increasing the affinity between the surfaces and the bacteria. In addition, they suggest that the binding of $Cd^{2+}$ ions by the carboxylic acid headgroups reduces the H-bonding of the groups; this reduction in the H-bonding reduced the energy barrier to changes in the polymer conformation and increased the corresponding color change. The proposed affect of the $Cd^{2+}$ ions on the chromic transition is consistent with the findings of Kew and Hall on the effect of cations on chromic changes caused by pH.[128]

We have used PDA coatings functionalized with anti-*E. coli* antibodies for the fluorescence detection of *E. coli*.[52] 10,12-PCDA liposomes were prepared with 0.5% fluorophore **19** incorporated and anti-E. coli antibodies conjugated to alkyl tails inserted by detergent dialysis. The unpolymerized liposomes were coated *via* filtration onto 0.45 μm mixed cellulose ester membranes in a 96-well filter plate and photopolymerized. The coatings were exposed to increasing doses of *E. coli* and control buffer with filtration and emission measurement between each dose. An emission response was detected for 100 *E. coli* per well; the emission of the coatings increased with number of *E. coli* filtered up to $\sim 10^4$/well (Fig. 10). Coatings exposed to the control buffer and repeated filtration showed a smaller increase in emission, suggesting some conversion by mechanical stress from the repeated filtration. The detection levels with our system are significantly lower than those presented above. Filtration leads to concentration of the bacteria at the coated surface increasing the sensitivity of the material response and potentially allowing detection of organisms in the larger volumes typically used in environmental analysis.

Jelinek and co-workers have recently described preliminary work on immobilization of PDA in agar for bacterial detection.[96] Unpolymerized mixed liposomes of 60/40 10,12-TRCDA/DMPC were mixed with hot Luria-Burtani agar and allowed to cool; whether the liposome structure survives this treatment was not determined. The TRCDA in the composite material was polymerized with UV light and formed blue PDA. Incubation of three different bacteria, including both Gram positive and negative, caused local changes in color and fluorescence of the embedded PDA at sites of bacteria growth. This approach does not permit identification of the bacteria species, but does reduce the time needed for detecting the presence of bacteria relative to visual detection of colonies.

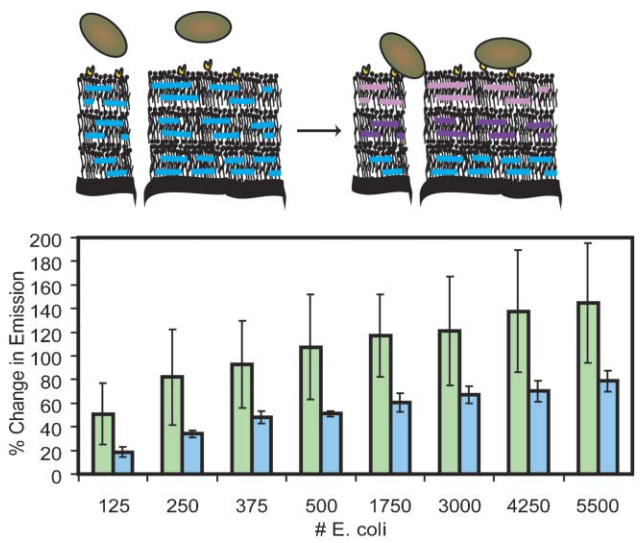


**Fig. 10** Cartoon and chart showing detection of *E. coli* filtered through PDA coatings with antibodies and **19** incorporated, deposited on nanoporous membranes. Green bars show response to filtration of the *E. coli* solution; blue bars show response to filtration of a control solution.

### 4.2 Detection of proteins

In general, the most widespread and convincing detection of bioanalytes with PDA systems has been of proteins that affect cell membranes, either through insertion, pore formation or enzymatic cleavage. Many proteins of interest, including some potential biowarfare agents, fall into these categories. In addition, detection of proteins binding to ligands – either small molecules or other proteins – has been demonstrated.

Following the demonstration of the colorimetric response of PDA materials incorporating sialic acid to influenza virus, Charych *et al*. investigated the detection of the B chain of cholera toxin (CTB) using similar materials and the ganglioside $GM_1$.[155] Pentameric CTB is known to bind to $GM_1$ at cell surfaces disrupting the lipid structure and allowing passage of the A chain of cholera toxin into the cell interior. They reported colorimetric detection of CTB at 40 μg $mL^{-1}$ (0.7 μM), with poly(10,12-PCDA) LB films incorporating 5% **22** and 5% $GM_1$. The $GM_1$ ligand was not polymerized into the PDA films, or covalently attached to the backbone; the authors hypothesized that binding of the CTB to the $GM_1$ was followed by partial insertion of the protein into the film that perturbed the PDA and caused the colorimetric change. Subsequently Pan and Charych developed PDA liposomes from poly(5,7-DCDA) with $GM_1$ that also changed color in the presence of CTB, but not when exposed to comparable amounts of other proteins.[156] The liposome assay, however, was not as sensitive as the film assay, detecting CTB at 0.1 mg $mL^{-1}$ (1.7 μM); despite this, Charych preferred liposomes because they had overall higher absorbance values and hence more easily measured color changes.[155] Comparable poly(10,12-PCDA)/$GM_1$ liposomes had a greatly reduced colorimetric response to CTB; Pan and Charych attributed the reduced response to the polymer being further from the headgroup. The response could also be affected by the overall longer diacetylene chain length compared to the poly(5,7-DCDA) based liposomes or by the polymer being an odd number of methylenes from the headgroups rather than an even number.

Cheng and co-workers later expanded on this work by preparing PDA monolayer films from 90% 10,12-PCDA with 5% **22** and 5% $GM_1$ incorporated and using them for the colorimetric detection of CTB.[150] The films showed a CR of 8% when exposed to 10 μg $mL^{-1}$ (0.17 μM) CTB, barely above the 5% background CR; the response to CTB then rose swiftly up to 60 μg $mL^{-1}$ and saturated above 100 μg $mL^{-1}$. The authors subsequently prepared multi-layer films from 40% of

bolaamphiphile 10,12-dodecadiyn-1,22-dioic acid (Scheme 3, **5**), 20% $GM_1$, 20% of a methylated dicysteine 10,12-PCDA derivative (Scheme 10, **23**) and 20% cholesterol; these films showed an improved CR of 36% when exposed to 10 μg $mL^{-1}$ CTB.

Detection of the action of phospholipase $A_2$ ($PLA_2$), which degrades lipid membranes, has also been quite successful. $PLA_2$ selectively cleaves the ester bond at the 2 position of the phospholipid glycerol backbone generating a free fatty acid and degrading the packing of the lipid membrane. Charych, Jelinek and co-workers first reported the colorimetric detection of $PLA_2$ using poly(10,12-TRCDA) liposomes incorporating DMPC.[77,157] $PLA_2$ activity was detected at 0.13 mg $mL^{-1}$ (9 μM) by colorimetric detection using 60% poly(10,12-TRCDA)/40% DMPC liposomes. The liposomes were studied with $^{31}P$, $^{13}C$ and $^{1}H$ NMR to characterize the DMPC in the liposomes initially, and to monitor the cleavage of the ester groups. The connection between lipid cleavage and PDA color change was confirmed by a parallel assay using a colored substrate, and by inhibition of the $PLA_2$. Exposure of the mixed PDA/DMPC liposomes to phospholipases C and D and to β-bungarotoxin also caused colorimetric changes.[77] TEM of the mixed PDA/DMPC liposomes before and after exposure to phospholipases showed cracking and pitting of the vesicles, suggesting significant morphological changes occurred upon the cleavage of the phospholipids.

Jelinek and co-workers subsequently compared the colorimetric response of PDA liposomes incorporating DMPC, cebroside, sphingomyelin and lipid extracts from *E. coli* and *Haloferax volcanii* to $PLA_2$, sphingomyelinase, and galactoside at 20 units/30 μL liposomes, and showed that the responses were enzyme/substrate specific.[158]

$PLA_2$ activity at 6 μM has also been detected through emission changes of 70% poly(10,12-TRCDA)/30% DMPC liposomes with and without fluorophore **18** incorporated.[137] A comparison of emission and colorimetric response demonstrated that the emission changes were much greater than the colorimetric response and that the addition of the fluorophore further increased the emission changes. $PLA_2$ activity down to 2.5 μM, and inhibition of 10 μM $PLA_2$ by 13 μM 12-*epi*-scalaradial (SLD), were recently detected with 60% poly(10,12-TRCDA)/33%DMPC/7% DPPT and 60% poly(6,8-DCDA)/33%DMPC/7% DPPT liposomes. The liposomes had 0.05% **18** incorporated and were attached to glass fiber membranes in 96-well plates.[101] It was seen (Fig. 11) that the poly(6,8-DCDA) based liposomes responded more to the action of the enzyme; the greater response could rise both from the reduced distance between the headgroups and the polymer and the shorter chain length. In general, the success of $PLA_2$ and other lipid-cleaving enzyme detection assays using mixed PDA/lipid liposomes arises from the enzyme amplification effect, and the extensive structural changes in the lipid region of the vesicles caused by the enzymatic activity of the target.

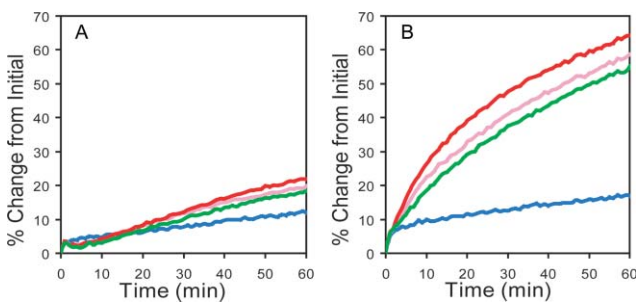


**Fig. 11** Change in emission at 640 nm of tethered PDA/DMPC liposomes with 10 μM $PLA_2$ (red), 2.5 μM $PLA_2$ (pink), 10 μM $PLA_2$ with 13 μM SLD (green) and blank with 13 μM SLD (blue). (A) poly(10,12-TRCDA)/DMPC/DPPT/**18**; (B) poly(6,8-DCDA)/DMPC/DPPT/**18**.

Streptolysin O (SLO), a pore forming toxin that binds to cholesterol, was detected at 2.5 nM by Ma and Cheng with polymerized vesicles prepared from 71% of the glycine derivative of 10,12-PCDA (**21**), 4% **15b** (Scheme 7) and 25% cholesterol.[159] Exposure of the vesicles to excess bovine serum albumin (BSA) and to tris(hydroxymethyl)aminomethane (TRIS) buffer, as controls, caused much smaller color changes, from blue to purple–blue rather than red. The authors examined the vesicles by DLS and TEM; DLS showed that the vesicle size increased upon reaction with SLO and TEM showed that the protein formed pores in the vesicles. The response was affected by the extent of polymerization of the vesicles. Too much UV irradiation led to non-responsive vesicles, presumably because of decrease in the fluidity of the membrane lipids arising from extensive polymer formation. The authors noted that the diacetylene PC **15b** was key to the colorimetric response; liposomes without the **15b** did not respond significantly to SLO, nor did liposomes containing 4% of saturated PCs. The authors speculated that **15b** disturbed the packing of the other diacetylenes reducing the barrier to chromic change; it may also have reduced polymerization increasing the fluidity of the liposomes. The vesicles had a CR of 30–35% with 2.5 nM SLO and a detection limit of ~0.1 nM. The sensitivity of the response is presumably due to extensive disruption of the vesicle caused by the protein (Fig. 12).

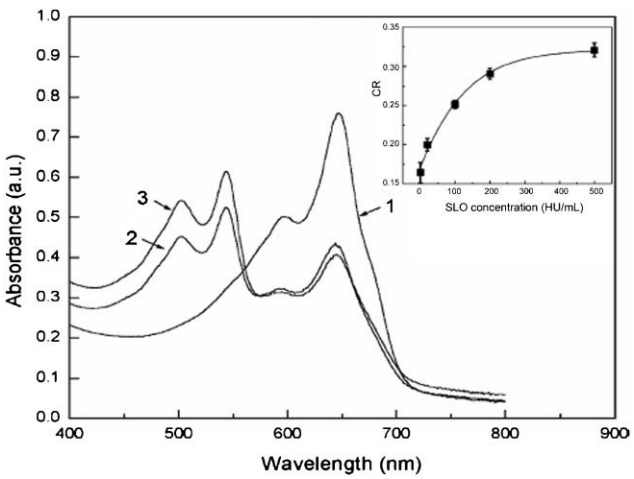


**Fig. 12** Absorption spectra for the PDA liposome sensors in response to SLO toxin. (1) original liposomes, (2) addition of 200 HU/mL SLO (~76 ng/mL), and (3) addition of 500 HU/mL SLO. Calibration plot of CR *vs.* SLO concentrations is inset, axes labels recreated for clarity. Reproduced with permission from ref. 159, Copyright 2005, American Chemical Society.

PDA materials have also been developed for proteins that bind to ligands without inserting into the membrane or cleaving lipids. These detection materials depend on perturbations caused by protein binding to ligands at the surfaces of the materials for signal generation, without having the membrane perturbation effects of the targets in the previously described assays.

Geiger *et al.* studied the multi-valent interaction of streptavidin with biotin incorporated in poly(10,12-PCDA) LB films, as a model system.[32] The films contained 10 wt% 10,12-PCDA amide linked to biotin *via* a short hydrophilic linker (Scheme 10, **24**). The authors discovered that they needed to stabilize the PDA monolayers on the aqueous subphase by addition of 1 mM $CdCl_2$, and to use a minimum of three PDA layers to obtain sufficient absorbance signal. In addition, they noted that the polymerized films were sensitive to buffers at pH 7.3, observing CR responses greater than 20% upon exposure of the films to TRIS/saline (50 mM TRIS/100–500 mM NaCl or KCl) buffers, and to phosphate buffered saline solutions. TRIS (50 mM) without additional NaCl or KCl caused a lower CR of 6–15%. It is possible that displacement of the $Cd^{2+}$ ions coordinated to the headgroups by the large excess of NaCl and KCl in the buffered saline solutions caused the color changes. The films were exposed to different concentrations of streptavidin with the response showing a hook effect: a significant CR of $\sim$65% was seen at a streptavidin : biotin ratio of 1 : 2; low CRs were observed for ratios of 1 : 3 and 1 : 1, and no CR detected above background for 1 : 4 streptavidin : biotin. These results were explained by the hypothesis that having one streptavidin to bind to two biotins attached at different points along the polymer backbone causes significant stress to the backbone and hence color change, whereas having one streptavidin bind to one biotin does not.

Several groups have used PDA liposomes for detection of antibodies. Jelinek, Kolusheva and co-workers reported colorimetric detection of antibodies with 60/40 poly(10,12-TRCDA)/DMPC liposomes incorporating 0.2% of a peptide composed of a membrane inserting hydrophobic sequence and a known epitope sequence of the antibody.[160] ELISA assays confirmed selective binding of the antibodies to their specific epitopes; however, the colorimetric responses of the liposomes were modest (20–35%), in particular given the relatively high concentrations on antibodies added (0.1–0.7 mg $mL^{-1}$). Santana and co-workers reported using 80/20 poly(10,12-TRCDA)/cardiolipin liposomes for the colorimetric detection of anti-cardiolipin antibodies; they saw CRs of 70–80% with 50 μg $mL^{-1}$ antibodies.[161] The increased response at lower antibody concentrations may be from the much higher percentage of antigen in the liposomes, as compared to the epitope peptides in the work by Kolusheva *et al.*The response was selective for the anti-cardiolipin antibodies over non-specific antibodies, with a sigmoidal response to increasing antibody concentration, attributed by the authors to the absorbed antibodies on the liposome surface exerting a cooperative effect in causing conformational changes. The authors also noted that purple-colored liposome solutions, with higher absorbances at 550 nm created by increased polymerization, were more responsive to low concentrations of antibody than blue liposomes, though the responses to higher concentrations of antibodies were similar.

Antibodies have been used as ligands in PDA materials for detection of other proteins. Gill and Ballesteros reported colorimetric detection of human α-fetoprotein (HAF) by 60/30/10 poly(2-aminoethyl 2,4-tricosadiynamide) [Scheme 10, **25**]/DMPC/1-linoleoyl-2-palmitoyl-*sn*-glycero-3-phosphoethanolamine (LPPE) liposomes conjugated to anti-HAF antibodies, both in solution, and with the liposomes encapsulated in mesoporous sol–gels.[95] The antibodies were conjugated to the liposomes using an NHS/maleimide heterobifunctional linker, but no effort was made to separate unreacted protein from the liposomes. The reported response of the liposomes to HAF was both swift and sensitive, taking 5 to 10 min to reach maximal CR, with detection limits of 0.1 ng $mL^{-1}$ HAF for the free liposomes and 0.4 ng $mL^{-1}$ HAF for the encapsulated liposomes. The encapsulated liposomes showed a reduced CR when compared to the free liposomes at all concentrations of HAF; however, the reported limits-of-detection of HAF for both the free and encapsulated liposomes are much lower than seen in other published PDA protein assays. The encapsulated liposomes did not respond significantly to 15 ng $mL^{-1}$ BSA. The authors also prepared homologous sol–gels with 5,7-DCDA, 5,7-TRCDA, 5,7-TCDA and 10,12-PCDA 2-aminoethyl derivatives in place of **25** and saw slower responses to HAF.

Jiang and co-workers prepared poly(10,12-TRCDA) suspensions with 0–40% DMPC incorporated and conjugated anti-human immunoglobulin (h-IgG) antibodies to the particles *via* conversion of the carboxylic acid headgroups to active NHS esters, which then reacted with the antibody surface amine groups.[79] Unreacted NHS groups were capped with BSA, but unreacted antibodies were not removed. The suspensions showed colorimetric detection of h-IgG at 1 ng $mL^{-1}$. TEM images of the antibody conjugated PDA materials before and after addition of the h-IgG show that PDA-antibody conjugates without DMPC are vesicles and aggregate after addition of the h-IgG, whereas materials prepared with 40% DMPC and conjugated to antibodies form flat sheets that also form larger aggregates/constructs after addition of h-IgG. The CR was increased by incorporation of DMPC; incubation with 10 ng $mL^{-1}$ h-IgG caused a CR of 27% for poly(10,12-TRCDA) and a CR of 41% for 60/40 poly(10,12-TRCDA)/DMPC. The response was slower than reported by Gill and Ballesteros, taking 20 min for a significant CR to develop, and the CR continuing to increase over 2 h. Comparison of the detection results presented in these two papers suggests that use of 2,4- rather than 10,12-tricosadiynes helps obtain a swift and sensitive response, though differences in head group and material composition probably also play a role.

Recently, Jelinek and co-workers have reported colorimetric detection of proteins with 60/40 poly(10,12-TRCDA)/DMPC liposomes mixed with calixarenes displaying ammonium, amine and phosphate groups.[162] The calixarenes were added to the liposomes post polymerization with the expectation that the hydrophobic portion inserts into DMPC domains. Proteins of different charges at 1 μg $mL^{-1}$ were added to the liposome/calixarene mixtures and the CR of the liposomes measured; the CR was compared to the CR of liposomes without calixarenes

added but with proteins. A correlation was drawn between the CR of the liposome-calixarene mixtures, the charge of the protein, and the charge of the calixarenes; the authors suggest that these systems could be used for "finger-printing" of proteins based on charge.

### 4.3 Detection of biologically relevant molecules

PDA liposomes incorporating proteins and/or phospholipids have also been used for detection of ions[158,163] and molecules. Cheng and Stevens, in pursuit of a glucose sensor, developed poly(10,12-PCDA) LB films with hexokinase, an enzyme that undergoes a conformational change upon binding glucose, attached to the film surface *via* amide bonds.[164] The LB films showed a modest colorimetric response upon exposure to 10 mM glucose; the authors hypothesized that the 8 Å conformational change of the hexokinase upon binding to glucose was too small to cause a large colorimetric change in the PDA film. It is also possible that the attachment of the enzyme at multiple points to the film raised the energy required for the protein's conformational change.

Rangin and Basu have reported colorimetric recognition of LPS characteristic of different bacteria using poly(10,12-PCDA) liposomes with 5% of 10,12-PCDA with tryptophan or tyrosine headgroups (Fig. 13).[165] The liposomes were exposed to 2.2 mg $mL^{-1}$ LPS obtained from five different gram-negative bacteria under different conditions: at room temperature, at 35 °C, combined with sodium dodecyl sulfate (SDS), or combined with ethylenediamine tetraacetic acid (EDTA). The authors noted that LPS from *Salmonella enteriditis* did not cause a response from either liposome formulation under any of the conditions, while LPS from *Salmonella minnesota* gave a significant response. The pattern of CR of the two different liposomes under the four different conditions formed a fingerprint that allowed identification of the bacterial source of the LPS in a blind test of the five types.

Jelinek, Schrader and co-workers have recently shown the fluorescence detection of catecholamines with a 60/40 poly(10,12-TRCDA)/DMPC liposome platform. The liposomes were combined with synthetic host compounds, designed to bind catecholamines, prior to addition of the targets.[147] The emission responses were dependent on the specific host added; a selective emission response was seen to 25 μM noradrenaline (~30%), and semi-selective responses of ~10–12% to 25 μM dopamine and 2-amino-1-phenylethanol. Addition of urine samples spiked with micromolar concentrations noradrenaline and dopamine also caused emission responses, suggesting that the detection method could be used on physiological samples.

PDA/phospholipid liposomes have also been proposed for detecting small molecule interactions with lipid membranes, including colorimetric screening of membrane penetration enhancers,[78] fluorescent screening for drug-like properties of compound libraries,[60] and colorimetric screening of interactions between drug compounds and lipid membranes.[166] The non-specific response of PDA liposomes (without phospholipids) to small molecules has also been proposed for the fluorescent determination of compound concentrations in screening assays.[167]

### 4.4 Other applications

PDA liposomes have also been used in more fundamental biochemical studies where detection was not the primary goal. For example, they have been used for the study of cell membrane phenomena, including stabilizing membrane proteins and as a platform for characterizing interactions of peptides, small molecules and viruses with membranes. In these studies, detection of an analyte was not the aim, though the color response of the liposomes was correlated to membrane interactions in some cases. The successful use of PDA materials in these applications provides further insights into how PDA materials can be better designed for biosensing purposes.

**4.4.1 Membrane proteins.** A major goal in early work with PDA liposomes was to use the polymerized liposomes as a stable matrix for membrane proteins. Ringsdorf and co-workers prepared delipidated ATP synthetase, which was inactive, then mixed it with pre-polymerized and unpolymerized liposomes (separately) prepared from a *N*,*N*-bis(10,12-HPCDA-ethyl)ammonium-*N*-ethylsulfate (Scheme 7, **14**). They saw the activity of the enzyme was restored both after mixing with polymerized liposomes and after mixing with unpolymerized liposomes that were then photopolymerized. The presence of the enzyme in the liposomes was confirmed by gel electrophoresis and the authors ascertained that the UV exposure did not affect the enzyme activity. The enzyme activity was highest (and equivalent to the activity in soybean lecithin liposomes) when mixed with liposomes that had been pre-polymerized for extended periods shifting the maximum absorbance peak below 500 nm, and the lowest when mixed with liposomes that had been briefly polymerized with the maximum absorbance around 550 nm. The authors attributed the increase in activity to structural rearrangements in the liposome bilayers upon extended polymerization. DSC of the

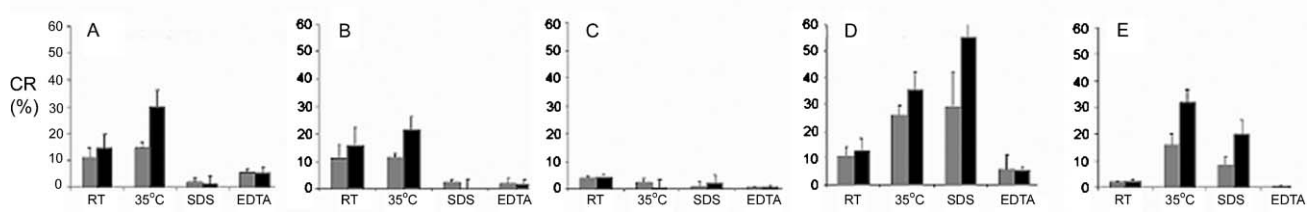


**Fig. 13** CR values obtained upon exposure of PDA liposome array with tryptophan (grey bars) and tyrosine (black bars) headgroups to LPS (2.2 mg $mL^{-1}$) from different Gram negative bacteria (A) *E. coli* O26:B6; (B) *Pseudomonas aeruginosa*; (C) *Salmonella enteriditis*; (D) *Salmonella minnesota*; (E) *Shigella flexneri*, at room temperature, at 35 °C, with SDS (2 mM), or with EDTA (1 mM). Reproduced with permission from ref. 165, Copyright 2004, American Chemical Society. Figure titles and axis labels recreated for clarity.

 

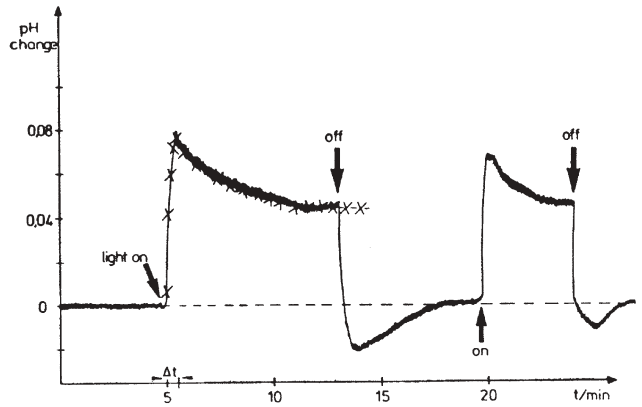


**Fig. 14** Proton pumping activity of bacteriorhodopsin (BR) in polymerized sulfolipid liposomes (BR: 150 μg $mL^{-1}$, sulfolipid: 0.6 mg $mL^{-1}$). Reproduced with permission from ref. 141, Copyright 1983, Elsevier Science Publishers.

polymerized liposomes showed that there were unpolymerized monomer domains in the polymerized liposomes; the authors presumed that the enzyme partitioned into those domains and was stabilized by the polymerized regions.

Subsequently, Ringsdorf and co-workers incorporated bacteriorhodopsin into liposomes made from **14**, in both the polymerized and unpolymerized state.[141] Bacteriorhodopsin is a light-activated (570 nm) proton pump; interestingly, the protein adopted a reverse orientation in the liposome. The activity of the protein was measured by monitoring the pH of the solution before, during and after light exposure; the activities in polymerized and unpolymerized liposomes were compared to each other and to the activity in soybean lecithin liposomes (Fig. 14). Up to 25 μg $mL^{-1}$ of bacteriorhodopsin, the activity of the protein was similar in all three systems; above that protein level the activity was higher in the lecithin liposomes, although the PDA and diacetylene liposomes had similar responses. The pH shifts in the polymerized liposomes were complicated by the liposomes responding to the 570 nm light used to activate the bacteriorhodopsin by becoming slightly leaky. The protein retained its activity upon storage in the polymerized liposomes, showing no change over a three month period, while the protein in the unpolymerized diacetylene liposomes had a ~33% loss of activity, and the protein in the lecithin liposomes lost all of its activity.

Lack of membrane fluidity makes pure PDA liposomes less suitable for most membrane proteins than natural lipid or mixed liposomes.[64] Research performed by Chapman and co-workers on the incorporation and photopolymerization of diacetylenes in bacteria cell membranes support this hypothesis.[168] *Acheloplasma laidlawii A* were grown on media enriched with diacetylene fatty acids; the bacteria incorporated the fatty acids into lipids in the cell membrane. Photopolymerization created PDA in the membranes and decreased the activity of NADH oxidase, a membrane bound protein, while the activity of ribonuclease, a protein associated with the membrane, but not incorporated in it, was unaffected.

**4.4.2 Membrane interactions.** Jelinek, Kolusheva and co-workers have used poly(10,12-TRCDA)/phospholipid liposomes to study the activity of membrane penetrating peptides at micro to millimolar concentrations. They prepared different liposomes varying the phospholipid composition[169] and also incorporating LPS,[170] and exposed them to known membrane inserting peptides and to analog peptides as controls. The interaction of the peptides with the liposomes was studied by measuring the CR, by surface fluorophore displacement, and by quenching assays. The peptides structures were also characterized by CD to show that the analogs lacked the full helical structures of the membrane inserting peptides.[171] The results of these studies were used to develop a model of the peptide liposome interactions, where the membrane inserting peptides partition into the phospholipid domains causing colorimetric changes. Non-inserting peptides can interact with surface groups and these surface interactions were observed to cause greater color changes than insertion in some cases.[170]

In recent work, Jelinek and co-workers describe the addition of PDA/phospholipid vesicles to cells and fluorescent microscopy studies of the cell/vesicle adjunct.[172] The vesicles adhere to the cell surfaces and reduce cell viability after two to three hours. The adhered vesicles were shown to respond with colorimetric and emission changes upon addition of small molecules[173] The addition of imipramine and quinidine to poly(10,12-TRCDA)/DMPE/DMPG labeled erythrocyte ghost cells caused an optical response detected both by fluorescent microscopy and UV-vis spectroscopy. Further control experiments are needed to determine whether the responses were due to the compounds interacting with the cell membranes, with the vesicles directly, or with both. The researchers did determine that addition of DPPE to the labeled cells caused a rise in emission whereas addition of DPPE to the free vesicles did not cause a colorimetric change. In a related study, the emission response of the PDA/phospholipid vesicles attached to Chinese hamster ovary (CHO) cells and exposed *vaccinia* virus was studied.[174] The response to the virus was dependent on the phospholipid composition; vesicles with DMPC showed the greatest response, and those with sphingomyelin and cholesterol the least. A similar pattern was seen for free PDA/phospholipid vesicles. Interestingly, the extent of the optical response showed an inverse trend to the amount of *vaccinia* virus inserting into the vesicles, as determined by other means. The authors propose that for poly(TRCDA)/DMPC vesicles the *vaccinia* virus interacts with the PDA portion of the vesicle, directly perturbing the polymer and causing the large optical change, and that for poly(TRCDA)/sphingomyelin/cholesterol vesicles the virus inserts into the phospholipid domains and has less effect on the polymer. This is consistent with the results previously seen with peptides by the Jelinek group and points to the desirability of using PDA materials with non-interactive headgroups to avoid non-specific responses.

### 4.5 Detection conclusions

These initial reports of detection of biological analytes with PDA materials are very encouraging; however, it should be noted that in many cases there has been as yet no follow up reports confirming the utility of these systems or demonstrating reproduction by other investigators.

Review of the PDA biosensing literature shows that there is no consensus on what the best material composition and forms are for target detection, though comparison of different results from multiple groups detecting the same target, suggest the PDA material composition is very important. In the detection both of *E. coli* and of antibodies, the use of 2,4-diacetylenes appears to lead to more responsive materials. Non-specific interactions between carboxylic acid headgroups of the commonly used diacetylene fatty acids and the amines of proteins can lead to non-specific responses. In some cases preparing PDA materials from diacetylene with non-ionizable headgroups may be preferable. Experimental parameters, including material preparation conditions, assay buffer composition, pH, and assay format, also strongly affect assay outcome.

Future challenges in the design of PDA biosensing materials include development of materials capable of reversible responses to biological targets, overall amplification of signal to increase sensitivity, and demonstration of selectivity against a wide variety of potential interferents.

## 5 Conclusion

In this article we have described different self-assembled PDA materials used in biosensing, discussed the current understanding of the mechanisms of optical change in PDA, and summarized the achievements to date of PDA sensing. PDA materials have been extensively studied over the last four decades; however, the field is still changing as new materials are developed, new signals are utilized and a better understanding of the basis of PDA responses is formed.

## Abbreviations

| | |
|---|---|
| AFM | Atomic force microscopy |
| BAM | Brewster angle microscopy |
| BSA | Bovine serum albumin |
| CD | Circular dichroism |
| CR | Colorimetric response |
| DCDA | Docosadiynoic acid |
| DLS | Dynamic light scattering |
| DMPC | 1,2-Dimyristoyl-*sn*-glycero-3-phosphocholine |
| DMPE | 1,2-Dimyristoyl-*sn*-glycero-3-phosphoethanolamine |
| DMPG | 1,2-Dimyristoyl-*sn*-glycero-3-phospho-1-glycerol |
| DPPE | 1,2-Dipalmitoyl-*sn*-glycero-3-phosphoethanolamine |
| DPPT | 1,2-Dipalmitoyl-*sn*-glycero-3-phosphothioethanol |
| DSC | Differential scanning calorimetry |
| ELISA | Enzyme-linked immunosorbent assay |
| ESR | Electron spin resonance |
| FTIR | Fourier-transform infrared spectroscopy |
| H-bond | Hydrogen bond |
| HCDA | Heneicosadiynoic acid |
| HEPES | 4-(2-Hydroxyethyl)-1-piperazineethanesulfonic acid |
| HPCDA | Heptacosadiynoic acid |
| LB | Langmuir–Blodgett |
| LPS | Lipopolysaccharide |
| LS | Langmuir–Schaefer |
| NHS | *N*-Hydroxysuccinimide |
| PC | Phosphatidylcholine |
| PCDA | Pentacosadiynoic acid |
| PDA | Polydiacetylene |
| P-EtOH | 2-Hydroxyethyl pentacosadiynamide |
| PLM | Polarized light microscopy |
| SAM | Self-assembled monolayer |
| SAXS | Small angle X-ray scattering |
| SEC | Size exclusion chromatography |
| SEM | Scanning electron microscopy |
| SERS | Surface enhanced Raman scattering |
| TCDA | Tetracosadiynoic acid |
| TEM | Transmission electron microscopy |
| TRCDA | Tricosadiynoic acid |
| TRIS | Tris(hydroxymethyl)aminomethane |
| UV | Ultraviolet |
| XRD | X-Ray diffraction |


## Acknowledgements

The authors thank Dr Choying Ni and Dr Zhibin Li, University of Delaware, W. M. Keck Electron Microscopy Facility for cryogenic TEM analysis of our attached liposomes/fibers. Unpublished results presented here were partially supported by a National Science Foundation SBIR Phase II grant DMI-0239587 and by an Army Research Office STTR Phase II contract W911NF-O4-C0132. The conclusions presented are of the authors alone and not endorsed by any government agency.


## References


1 G. Wegner, *Z. Naturforsch., Teil B*, 1969, **24**, 824–832.
2 B. Tieke, *Adv. Polym. Sci.*, 1985, **17**, 79–151.
3 *Polydiacetylenes*, ed. D. Bloor and R. R. Chance, Martinus Nijhoff Publishers, Boston, FL, 1985.
4 S. Okada, S. Peng, W. Spevak and D. H. Charych, *Acc. Chem. Res.*, 1998, **31**, 229–239.
5 H. Ribi, *US Pat.*, 5,622,872, 1995.
6 H. Ribi, T. Guion and P. T. Shafer, *US Pat.*, 5,491,097, 1994.
7 R. W. Carpick, D. Y. Sasaki, M. S. Marcus, M. A. Eriksson and A. R. Burns, *J. Phys.: Condens. Matter*, 2004, **16**, R679–R697.
8 H. Ringsdorf, B. Schlarb and J. Venzmer, *Angew. Chem., Int. Ed. Engl.*, 1988, **27**, 113–158.
9 D. F. O'Brien, B. Armitage, A. Benedicto, D. E. Bennet, H. G. Lamparksi, Y.-S. Lee, W. Srisri and T. M. Sisson, *Acc. Chem. Res.*, 1998, **31**, 861–868.
10 D. T. McQuade, A. E. Pullen and T. M. Swager, *Chem. Rev.*, 2000, **100**, 2537–2574.
11 W. Zhou, Y. Li and D. Zhu, *Chem. Asian J.*, 2007, **2**, 222–229.
12 G. Odian, *Principles of Polymerization*, John Wiley & Sons, Inc., New York, 3rd edn, 1991.
13 S. R. Sheth and D. E. Leckband, *Langmuir*, 1997, **13**, 5652–5662.
14 J. Morgan, G. Rumbles, B. Crystall, T. A. Smith and D. Bloor, *Chem. Phys. Lett.*, 1992, **196**, 455–461.
15 D. Bloor and M. R. Worboys, *J. Mater. Chem.*, 1998, **8**, 903–912.
16 B. Tieke and G. Lieser, *J. Colloid Interface Sci.*, 1982, **88**, 471–486.
17 G. J. Exarhos, W. M. Risen and R. H. Baughman, *J. Am. Chem. Soc.*, 1976, **98**, 481–487.
18 A. J. Campbell, C. K. L. Davies and D. N. Batchelder, *Macromol. Chem. Phys.*, 1998, **199**, 109–122.

19 V. Enklemann and J. B. Lando, *Acta Crystallogr., Sect. B*, 1978, **34**, 2352–2353.
20 R. F. Fischetti, M. Filipkowski, A. F. Garito and J. K. Blasie, *Phys. Rev. B*, 1988, **37**, 4714–4726.
21 C. Plachetta and R. C. Schulz, *Makromol. Chem., Rapid Commun.*, 1982, **3**, 815–819.
22 A. D. Nava, M. Thakur and A. E. Tonelli, *Macromolecules*, 1990, **23**, 3055–3063.
23 D. Lee, S. K. Sahoo, A. L. Cholli and D. J. Sandman, *Macromolecules*, 2002, **35**, 4347–4355.
24 R. R. Chance, R. H. Baughman, H. Müller and C. J. Eckhardt, *J. Chem. Phys.*, 1977, **67**, 3616–3618.
25 H. Eckhardt, D. S. Boudreaux and R. R. Chance, *J. Chem. Phys.*, 1986, **85**, 4116–4119.
26 V. Dobrosavljevic and R. M. Stratt, *Phys. Rev. B*, 1987, **35**, 2781–2794.
27 K. Kuriyama, H. Kikuchi and T. Kajiyama, *Langmuir*, 1998, **14**, 1130–1138.
28 G. Eglington and W. McRae, *Adv. Org. Chem.*, 1963, **4**, 252–281.
29 H. Tachibana, Y. Yamanaka, H. Sakai, M. Abe and M. Matsumoto, *Macromolecules*, 1999, **32**, 8306–8309.
30 H. Menzel, S. Horstmann, M. D. Mowery, M. Cai and C. E. Evans, *Polymer*, 2000, **41**, 8113–8119.
31 H. Menzel, M. D. Mowery, M. Cai and C. E. Evans, *J. Phys. Chem. B*, 1998, **102**, 9550–9556.
32 E. Geiger, P. Hug and B. A. Keller, *Macromol. Chem. Phys.*, 2002, **203**, 2422–2431.
33 T. E. Wilson and M. D. Bednarski, *Langmuir*, 1992, **8**, 2361–2364.
34 A. A. Deckert, J. C. Horne, B. Valentine, L. Kiernan and L. Fallon, *Langmuir*, 1995, **11**, 643–649.
35 S. Wang, R. Lunn, M. P. Krafft and R. M. Leblanc, *Langmuir*, 2000, **16**, 2882–2886.
36 S. Wang, J. Ramirez, Y. Chen, P. G. Wang and R. M. Leblanc, *Langmuir*, 1999, **15**, 5623–5629.
37 F. Gaboriaud, R. Golan, R. Volinsky, A. Berman and R. Jelinek, *Langmuir*, 2001, **17**, 3651–3657.
38 R. Volinsky, F. Gaboriaud, A. Berman and R. Jelinek, *J. Phys. Chem. B*, 2002, **106**, 9231–9236.
39 M. Shibata, F. Kaneko, M. Aketagawa and S. Kobayashi, *Thin Solid Films*, 1989, **179**, 433–437.
40 S. J. Johnson, R. W. Tillmann, T. A. Saul, B. L. Liu, P. M. Kenney, J. S. Daulton, H. E. Gaub and H. O. Ribi, *Langmuir*, 1995, **11**, 1257–1260.
41 Q. Huo, K. C. Russell and R. M. Leblanc, *Langmuir*, 1999, **15**, 3972–3980.
42 Q. Huo, S. Wang, A. Pisseloup, D. Verma and R. M. Leblanc, *Chem. Commun.*, 1999, 1601–1602.
43 D. J. Ahn, E.-H. Chae, G. S. Lee, H.-Y. Shim, T.-E. Chang, K.-D. Ahn and J.-M. Kim, *J. Am. Chem. Soc.*, 2003, **125**, 8976–8977.
44 F. Gaboriaud, R. Volinsky, A. Berman and R. Jelinek, *J. Colloid Interface Sci.*, 2005, **287**, 191–197.
45 S. P. Sullivan, A. Schnieders, S. K. Mbugua and T. P. J. Beebe, *Langmuir*, 2005, **21**, 1322–1327.
46 D. N. Batchelder, S. D. Evans, T. L. Freeman, L. Haussling, H. Ringsdorf and H. Wolf, *J. Am. Chem. Soc.*, 1994, **116**, 1050–1053.
47 T. Kim, R. M. Crooks, M. Tsen and L. Sun, *J. Am. Chem. Soc.*, 1995, **117**, 3963–3967.
48 T. Kim, Q. Ye, L. Sun, K. C. Chan and R. M. Crooks, *Langmuir*, 1996, **12**, 6065–6073.
49 T. Kim, K. C. Chan and R. M. Crooks, *J. Am. Chem. Soc.*, 1997, **119**, 189–193.
50 M. D. Mowery, H. Menzel, M. Cai and C. E. Evans, *Langmuir*, 1998, **14**, 5594–5602.
51 M. A. Reppy, S. A. Sporn and C. F. Saller, *US Pat.*, 6,984,528, 2000.
52 B. A. Pindzola, A. T. Nguyen and M. A. Reppy, *Chem. Commun.*, 2006, 906–908.
53 T. Kuo and D. F. O'Brien, *J. Am. Chem. Soc.*, 1988, **110**, 7571–7572.
54 T. Kuo and D. F. O'Brien, *Macromolecules*, 1990, **23**, 3225–3230.
55 T. Kuo and D. F. O'Brien, *J. Chem. Soc., Chem. Commun.*, 1990, 839–841.
56 T. Kuo and D. F. O'Brien, *Langmuir*, 1991, **7**, 584–589.
57 D. G. Rhodes, D. A. Frankel, T. Kuo and D. F. O'Brien, *Langmuir*, 1994, **10**, 267–275.
58 G. Wang and R. I. Hollingsworth, *Langmuir*, 1999, **15**, 3062–3069.
59 D. G. Rhodes, Z. Xu and R. Bittman, *Biochem. Biophys. Acta*, 1992, **1128**, 93–104.
60 M. A. Reppy and C. F. Saller, *US Pat.*, 20040023303, 2003.
61 G. T. Hermanson, *Bioconjugate Techniques*, Academic Press, Inc., San Diego, CA, 1996.
62 D. Day, H.-H. Hub and H. Ringsdorf, *Isr. J. Chem.*, 1979, **18**, 325–329.
63 H. Bader, K. Dorn, B. Hupfer and H. Ringsdorf, *Adv. Polym. Sci.*, 1985, **64**, 1–62.
64 B. Hupfer, H. Ringsdorf and H. Schupp, *Chem. Phys. Lipids*, 1983, **33**, 355–374.
65 H.-H. Hub, B. Hupfer, H. Koch and H. Ringsdorf, *Angew. Chem., Int. Ed. Engl.*, 1980, **19**, 938–940.
66 N. Wagner, K. Dose, H. Koch and H. Ringsdorf, *FEBS Lett.*, 1981, **132**, 313–318.
67 D. S. Johnston, S. Sanghera, M. Pons and D. Chapman, *Biochem. Biophys. Acta*, 1980, **602**, 57–69.
68 M. Pons, D. S. Johnston and D. Chapman, *Biochem. Biophys. Acta*, 1982, **693**, 461–465.
69 J. Leaver, A. Alonso, A. A. Durrani and D. Chapman, *Biochem. Biophys. Acta*, 1983, **732**, 210–218.
70 A. Singh, R. B. Thompson and J. M. Schnur, *J. Am. Chem. Soc.*, 1986, **108**, 2785–2787.
71 H. Bader, H. Ringsdorf and J. Skura, *Angew. Chem., Int. Ed. Engl.*, 1981, **20**, 91–92.
72 H. Bader and H. Ringsdorf, *J. Polym. Sci.: Polym. Chem. Ed.*, 1982, **20**, 1623–1628.
73 H. Bader and H. Ringsdorf, *Faraday Discuss. Chem. Soc.*, 1986, **81**, 329–337.
74 E. Lopez, D. F. O'Brien and T. H. Whitesides, *J. Am. Chem. Soc.*, 1982, **104**, 305–307.
75 B. M. Peek, J. H. Callahan, K. Namboodiri, A. Singh and B. P. Gaber, *Macromolecules*, 1994, **27**, 292–297.
76 S. Kolusheva, E. Wachtel and R. Jelinek, *J. Lipid Res.*, 2003, **44**, 65–71.
77 R. Jelinek, S. Okada, S. Norvez and D. H. Charych, *Chem. Biol.*, 1998, **5**, 619–629.
78 D. Evard, E. Touitou, S. Kolusheva, Y. Fishov and R. Jelinek, *Pharm. Res.*, 2001, **18**, 943–949.
79 Y.-l. Su, J.-r. Li and L. Jiang, *Colloids Surf., B*, 2004, **38**, 29–33.
80 J. M. Schnur, R. Price, P. Schoen, P. Yager, J. M. Calvert, J. Georger and A. Singh, *Thin Solid Films*, 1987, **152**, 181–206.
81 A. L. Plant, D. M. Benson and G. L. Trusty, *Biophys. J.*, 1990, **57**, 925–933.
82 G. Wang and R. I. Hollingsworth, *Langmuir*, 1999, **15**, 6135–6138.
83 D. A. Frankel and D. F. O'Brien, *J. Am. Chem. Soc.*, 1994, **116**, 10057–10069.
84 G. Wang and R. I. Hollingsworth, *Adv. Mater.*, 2000, **12**, 871–874.
85 Q. Cheng, M. Yamamoto and R. C. Stevens, *Langmuir*, 2000, **16**, 5333–5342.
86 J. Song, Q. Cheng, S. Kopta and R. C. Stevens, *J. Am. Chem. Soc.*, 2001, **123**, 3205–3213.
87 J. Song, Q. Cheng and R. C. Stevens, *Chem. Phys. Lipids*, 2002, **2002**, 203–214.
88 J. Song, J. S. Cisar and C. R. Bertozzi, *J. Am. Chem. Soc.*, 2004, **126**, 8459–8465.
89 J. M. Schnur, B. R. Ratna, J. V. Selinger, A. Singh, G. Jyothi and K. R. K. Easwaran, *Science*, 1994, **264**, 945–947.
90 S. Pakhomov, R. P. Hammer, B. K. Mishra and B. N. Thomas, *Proc. Natl. Acad. Sci. USA*, 2003, **100**, 3040–3042.
91 S. B. Lee, R. Koepsel, D. B. Stolz, H. E. Warriner and A. J. Russell, *J. Am. Chem. Soc.*, 2004, **126**, 13400–13405.
92 S. B. Lee, R. R. Koepsel and A. J. Russell, *Nano Lett.*, 2005, **5**, 2202–2206.
93 M. A. Reppy, B. A. Pinzola and E. Cleveland, unpublished results.
94 S. A. Yamanaka, D. H. Charych, D. A. Loy and D. Y. Sasaki, *Langmuir*, 1997, **13**, 5049–5053.
95 I. Gill and A. Ballesteros, *Angew. Chem., Int. Ed.*, 2003, **42**, 3264–3267.
96 L. Silbert, I. Ben Shlush, E. Israel, A. Porgador, S. Kolusheva and R. Jelinek, *Appl. Environ. Microbiol.*, 2006, **72**, 7339–7344.

97 I. Stanish, J. P. Santos and A. Singh, *J. Am. Chem. Soc.*, 2001, **123**, 1008–1009.
98 J.-M. Kim, E.-K. Ji, S. M. Woo, H. Lee and D. J. Ahn, *Adv. Mater.*, 2003, **15**, 1118–1121.
99 H.-Y. Shim, S. H. Lee, D. J. Ahn, K.-D. Ahn and J.-M. Kim, *Mater. Sci. Eng., C*, 2004, **24**, 157–161.
100 J.-M. Kim, Y. B. Lee, D. H. Yang, J.-S. Lee, G. S. Lee and D. J. Ahn, *J. Am. Chem. Soc.*, 2005, **127**, 17580–17581.
101 M. A. Reppy and B. A. Pindzola, *Mater. Res. Soc. Symp. Proc.*, 2006, **942**, W13_10–W13_15.
102 P. N. Prasad and D. J. Williams, in *Introduction of Nonlinear Optical Effects in Molecules & Polymers*, John Wiley & Sons, New York, 1981, pp. 231–235.
103 A. A. Deckert, L. Fallon, L. Kiernan, C. Cashin, A. Perrone and T. Encalarde, *Langmuir*, 1994, **10**, 1948–1954.
104 R. W. Carpick, T. M. Mayer, D. Y. Sasaki and A. R. Burns, *Langmuir*, 2000, **16**, 4639–4647.
105 O. J. Dautel, M. Robitzer, J.-P. Lère-Porte, F. Serein-Spirau and J. J. E. Moreau, *J. Am. Chem. Soc.*, 2006, **128**, 16213–16223.
106 B. Chu and R. Xu, *Acc. Chem. Res.*, 1991, **24**, 384–389.
107 H. Oikawa, T. Korenaga, S. Okada and H. Nakanishi, *Polymer*, 1999, **40**, 5993–6001.
108 S. J. Kew and E. A. H. Hall, *J. Mater. Chem.*, 2006, **16**, 2039–2047.
109 C. W. Yuan, C. L. Lu, Y. Liang, N. Gu and Y. Wei, *Solid State Commun.*, 1991, **80**, 493–495.
110 J. Yoon, S. K. Chae and J.-M. Kim, *J. Am. Chem. Soc.*, 2007, **129**, 3038–3039.
111 R. H. Baughman and R. R. Chance, *J. Polym. Sci., Part B: Polym. Phys.*, 1976, **14**, 2037–2045.
112 S. Suhai, *Phys. Rev. Lett. B*, 1984, **29**, 4570–4581.
113 B. J. Orchard and S. K. Tripathy, *Macromolecules*, 1986, **19**, 1844–1850.
114 R. Lecuiller, J. Berrehar, C. Lapersonne-Meyer and M. Schott, *Phys. Rev. Lett.*, 1998, **80**, 4068–4071.
115 R. Lecuiller, J. Berrehar, C. Lapersonne-Meyer, M. Schott and J.-D. Ganiere, *Chem. Phys. Lett.*, 1999, **314**, 255–260.
116 R. Lecuiller, J. Berrehar, D. Ganiere, C. Lapersonne-Meyer and M. Schott, *Phys. Rev. B*, 2002, **66**, 125205.
117 F. Dubin, J. Berrehar, R. Grousson, T. Guillet, C. Lapersonne-Meyer, M. Schott and V. Voliotis, *Phys. Rev. B*, 2002, **66**, 113202.
118 M. Schott, *Synth. Met.*, 2003, **139**, 739–742.
119 M. Schott, *J. Phys. Chem. B*, 2006, **110**, 15864–15868.
120 D. T. McQuade, J. Kim and T. M. Swager, *J. Am. Chem. Soc.*, 2000, **122**, 5885–5886.
121 Y. Tomioka, N. Tanaka and S. Imazeki, *J. Chem. Phys.*, 1989, **91**, 5694–5700.
122 N. Mino, H. Tamura and K. Ogawa, *Langmuir*, 1991, **7**, 2336–2341.
123 A. Lio, A. Reichert, J. O. Nagy, M. B. Salmeron and D. H. Charych, *J. Vac. Sci. Technol., B*, 1996, **14**, 1481–1485.
124 A. Lio, A. Reichert, D. J. Ahn, J. O. Nagy, M. B. Salmeron and D. H. Charych, *Langmuir*, 1997, **13**, 6524–6532.
125 N. Mino, H. Tamura and K. Ogawa, *Langmuir*, 1992, **8**, 594–598.
126 Q. Cheng and R. C. Stevens, *Langmuir*, 1998, **14**, 1974–1976.
127 U. Jonas, K. Shah, S. Norvez and D. H. Charych, *J. Am. Chem. Soc.*, 1999, **121**, 4580–4588.
128 S. J. Kew and E. A. H. Hall, *Anal. Chem.*, 2006, **78**, 2231–2238.
129 N. Mino, H. Tamura and K. Ogawa, *Langmuir*, 1991, **7**, 2336–2341.
130 K. Kuriyama, H. Kikuchi and T. Kajiyama, *Langmuir*, 1996, **12**, 2283–2288.
131 R. W. Carpick, D. Y. Sasaki and A. R. Burns, *Langmuir*, 2000, **16**, 1270–1278.
132 A. R. Burns, R. W. Carpick, D. Y. Sasaki, J. A. Shelnutt and R. Haddad, *Tribol. Lett.*, 2001, **10**, 89–96.
133 D. H. Charych, J. O. Nagy, W. Spevak and M. D. Bednarski, *Science*, 1993, **261**, 585–588.
134 A. Yasuda, M. Yoshizawa and T. Kobayashi, *Chem. Phys. Lett.*, 1993, **209**, 281–286.
135 T. Kobayashi, M. Yasuda, S. Okada, H. Matsuda and H. Nakanishi, *Chem. Phys. Lett.*, 1997, **267**, 472–480.
136 J. I. Olmsted and M. Strand, *J. Phys. Chem.*, 1983, **87**, 4790–4792.
137 M. A. Reppy, *Mater. Res. Soc. Symp. Proc.*, 2002, **723**, O5_9_1–O5_9_6.
138 M. A. Reppy, unpublished results.
139 G. Ma, A. M. Muller, C. J. Bardeen and Q. Cheng, *Adv. Mater.*, 2006, **18**, 55–60.
140 H. Bader, R. van Wagenen, J. D. Andrade and H. Ringsdorf, *J. Colloid Interface Sci.*, 1984, **101**, 246–249.
141 R. Pabst, H. Ringsdorf, H. Koch and K. Dose, *FEBS Lett.*, 1983, **154**, 5–9.
142 P. N. Tyminski, L. H. Latimer and D. F. O'Brien, *J. Am. Chem. Soc.*, 1985, **107**, 7769–7770.
143 P. N. Tyminski, L. H. Latimer and D. F. O'Brien, *Biochemistry*, 1988, **27**, 2696–2705.
144 D. H. Charych, W. Spevak, J. O. Nagy and M. D. Bednarski, *Mater. Res. Soc. Symp. Proc.*, 1993, **292**, 153–161.
145 T. Peng, Q. Cheng and R. C. Stevens, *Anal. Chem.*, 2000, **72**, 1611–1617.
146 T. Saul, G. Der-Balain, P. Kenhey, H. Mathis, S. Johnson, H. Ribbi and T. Witty, *US Pat.*, 5,415,999, 1993.
147 S. Kolusheva, O. Molt, M. Herm, T. Schrader and R. Jelinek, *J. Am. Chem. Soc.*, 2005, **127**, 10000–10001.
148 A. Reichert, J. O. Nagy, W. Spevak and D. H. Charych, *J. Am. Chem. Soc.*, 1995, **117**, 829–830.
149 W. Spevak, J. O. Nagy, D. H. Charych, M. E. Schaefer, J. H. Gilbert and M. D. Bednarski, *J. Am. Chem. Soc.*, 1993, **115**, 1146–1147.
150 J. Song, Q. Cheng, S. Zhu and R. C. Stevens, *Biomed. Microdevices*, 2002, **4**, 213–221.
151 Z. Ma, J. Li, M. Liu, J. Cao, Z. Zou, J. Tu and L. Jiang, *J. Am. Chem. Soc.*, 1998, **120**, 12678–12679.
152 Z. F. Ma, J. R. Li, L. Jiang, J. Cao and P. Boullanger, *Langmuir*, 2000, **16**, 7801–7804.
153 Y. Zhang, Y. Fan, C. Sun, D. Shen, Y. Li and J. Li, *Colloids Surf., B*, 2005, **40**, 137–142.
154 Y. Zhang, B. Ma, Y. Li and J. Li, *Colloids Surf., B*, 2004, **35**, 41–44.
155 D. H. Charych, Q. Cheng, A. Reichert, G. Kuziemko, M. Stroh, J. O. Nagy, W. Spevak and R. C. Stevens, *Chem. Biol.*, 1996, **3**, 113–120.
156 J. Pan and D. H. Charych, *Langmuir*, 1996, **13**, 1365–1367.
157 S. Okada, R. Jelinek and D. H. Charych, *Angew. Chem., Int. Ed.*, 1998, **38**, 655–659.
158 S. Rozner, S. Kolusheva, Z. Cohen, W. Dowhan, J. Eichler and R. Jelinek, *Anal. Biochem.*, 2003, **319**, 96–104.
159 G. Ma and Q. Cheng, *Langmuir*, 2005, **21**, 6123–6126.
160 S. Kolusheva, R. Kafri and R. Jelinek, *J. Am. Chem. Soc.*, 2001, **123**, 417–422.
161 E. C. M. Cabral, P. T. Hennies, C. R. D. Correia, R. L. Zollner and M. H. A. Santana, *J. Liposome Res.*, 2003, **13**, 199–211.
162 S. Kolusheva, R. Zadmard, T. Schrader and R. Jelinek, *J. Am. Chem. Soc.*, 2006, **128**, 13592–13598.
163 S. Kolusheva, T. Shahal and R. Jelinek, *J. Am. Chem. Soc.*, 2000, **122**, 776–780.
164 Q. Cheng and R. C. Stevens, *Adv. Mater.*, 1997, **9**, 481–483.
165 M. Rangin and A. Basu, *J. Am. Chem. Soc.*, 2004, **126**, 5038–5039.
166 M. Katz, I. Ben-Shlush, S. Kolusheva and R. Jelinek, *Pharm. Res.*, 2006, **23**, 580–588.
167 M. A. Reppy and C. F. Saller, *US Pat.*, 20060051875, 2005.
168 J. Leaver, A. Alonso, A. Durrani and D. Chapman, *Biochem. Biophys. Acta*, 1983, **727**, 327–335.
169 S. Kolusheva, L. Boyer and R. Jelinek, *Nat. Biotechnol.*, 2000, **18**, 225–227.
170 R. Halvey, A. Rozek, S. Kolusheva, R. E. W. Hancock and R. Jelinek, *Peptides*, 2003, **24**, 1753–1761.
171 S. Kolusheva, T. Shahal and R. Jelinek, *Biochemistry*, 2000, **39**, 15851–15859.
172 Z. Orynbayeva, S. Kolusheva, E. Linveh, A. Lichtenshtein, I. Nathan and R. Jelinek, *Angew. Chem., Int. Ed.*, 2005, **44**, 1092–1096.
173 E. Shtelman, A. Tomer, S. Kolusheva and R. Jelinek, *Anal. Biochem.*, 2006, **348**, 151–153.
174 Z. Orynbayeva, S. Kolusheva, N. Groysman, N. Gavrielov, L. Lobel and R. Jelinek, *J. Virol.*, 2007, **81**, 1140–1147.
175 T. Itoh, T. Shichi, T. Yui and K. Takagi, *Langmuir*, 2005, **21**, 3217–3220.


 